REFERENCES

1. Kawai K. Screening for gastric cancer in Japan. *Clin. Gastroenterol.* 1978; **7**: 605–22.
2. Ohata H, Oka M, Yanaoka K *et al.* Gastric cancer screening of a high-risk population in Japan using serum pepsinogen and barium digital radiography. *Cancer Sci.* 2005; **96**: 713–20.
3. Enomoto S, Maekita T, Ohata H, Yanaoka K, Oka M, Ichinose M. Novel risk markers for gastric cancer screening: Present status and future prospects. *World J. Gastrointest. Endosc.* 2010; **2**: 381–7.
4. Campo R, Montserrat A, Brullet E. Transnasal gastroscopy compared to conventional gastroscopy: A randomized study of feasibility, safety, and tolerance. *Endoscopy* 1998; **30**: 448–52.
5. Roy JF, Duforest D, Marek TA. Prospective comparison of nasal versus oral insertion of a thin video endoscope in healthy volunteers. *Endoscopy* 1996; **28**: 422–4.
6. Christensen M, Achiam M, Trap R, Stockel M, Rosenberg J, Schulze S. Transnasal gastroscopy. *Dan. Med. Bull.* 2000; **47**: 218–20.
7. Dumortier J, Napoleon B, Hedelius F *et al.* Unsedated transnasal EGD in daily practice: Results with 1100 consecutive patients. *Gastrointest. Endosc.* 2003; **57**: 198–204.
8. Tack J, Talley NJ, Camilleri M *et al.* Functional gastroduodenal disorders. *Gastroenterology* 2006; **130**: 1466–79.
9. Brun R, Kuo B. Functional dyspepsia. *Therap. Adv. Gastroenterol.* 2010; **3**: 145–64.
10. Bredenoord AJ, Chial HJ, Camilleri M, Mullan BP, Murray JA. Gastric accommodation and emptying in evaluation of patients with upper gastrointestinal symptoms. *Clin. Gastroenterol. Hepatol.* 2003; **1**: 264–72.
11. Tack J, Piessevaux H, Coulie B, Caenepeel P, Janssens J. Role of impaired gastric accommodation to a meal in functional dyspepsia. *Gastroenterology* 1998; **115**: 1346–52.
12. Talley NJ, Locke GR 3rd, Lahr BD *et al.* Functional dyspepsia, delayed gastric emptying, and impaired quality of life. *Gut* 2006; **55**: 933–9.
13. Kindt S, Tack J. Impaired gastric accommodation and its role in dyspepsia. *Gut* 2006; **55**: 1685–91.
14. Keefe EB. Towards safer endoscopy. In: Cotton PB, Tytgat GNJ, Williams CB, Bowling TE (eds). *Annual of Gastrointestinal Endoscopy*. London: Rapid Science Publisher, 1997; 1–14.
15. Fass R. Symptom assessment tools for gastroesophageal reflux disease (GERD) treatment. *J. Clin. Gastroenterol.* 2007; **41**: 437–44.
16. Kusano M, Shimoyama Y, Sugimoto S *et al.* Development and evaluation of FSSG: Frequency scale for the symptoms of GERD. *J. Gastroenterol.* 2004; **39**: 888–91.
17. Kusano M, Shimoyama Y, Kawamura O *et al.* Proton pump inhibitors improve acid-related dyspepsia in gastroesophageal reflux disease patients. *Dig. Dis. Sci.* 2007; **52**: 1673–7.
18. Miyamoto M, Haruma K, Takeuchi K, Kuwabara M. Frequency scale for symptoms of gastroesophageal reflux disease predicts the need for addition of prokinetics to proton pump inhibitor therapy. *J. Gastroenterol. Hepatol.* 2008; **23**: 746–51.
19. Enomoto S, Oka M, Ohata H *et al.* Assessment of gastroesophageal reflux disease by serodiagnosis of Helicobacter pylori-related chronic gastritis stage. *World J. Gastrointest. Endosc.* 2011; **3**: 71–7.
20. Armstrong D, Bennett JR, Blum AL *et al.* The endoscopic assessment of esophagitis: A progress report on observer agreement. *Gastroenterology* 1996; **111**: 85–92.
21. Tarcin O, Gurbuz AK, Pocan S, Keskin O, Demirturk L. Acustimulation of the Neiguan point during gastroscopy: Its effects on nausea and retching. *Turk. J. Gastroenterol.* 2004; **15**: 258–62.
22. De Schepper HU, Cremonini F, Chitkara D, Camilleri M. Assessment of gastric accommodation: Overview and evaluation of current methods. *Neurogastroenterol. Motil.* 2004; **16**: 275–85.
23. Zaman A, Hahn M, Hapke R, Knigge K, Fennerty MB, Katon RM. A randomized trial of peroral versus transnasal unsedated endoscopy using an ultrathin videoendoscope. *Gastrointest. Endosc.* 1999; **49**: 279–84.
24. Watanabe H, Watanabe N, Ogura R *et al.* A randomized prospective trial comparing unsedated endoscopy via transnasal and transoral routes using 5.5-mm video endoscopy. *Dig. Dis. Sci.* 2009; **54**: 2155–60.
25. Trevisani L, Cifala V, Sartori S, Gilli G, Matarese G, Abbasciano V. Unsedated ultrathin upper endoscopy is better than conventional endoscopy in routine outpatient gastroenterology practice: A randomized trial. *World J. Gastroenterol.* 2007; **13**: 906–11.
26. Collins SL, Moore RA, McQuay HJ. The visual analogue pain intensity scale: What is moderate pain in millimetres? *Pain* 1997; **72**: 95–7.

© 2012 The Authors
Digestive Endoscopy © 2012 Japan Gastroenterological Endoscopy Society

Digestive Endoscopy (2012) **24**, 488 doi:10.1111/j.1443-1661.2012.01362.x

LETTERS, TECHNIQUES AND IMAGES

Phlegmonous gastritis caused by endoscopic ultrasound-guided fine-needle aspiration (EUS-FNA)

Phlegmonous gastritis (PG) is a rare, often fatal, condition characterized by suppurative bacterial infection of the stomach.[1] Mucosal damage of the stomach, alcoholism and an immunocompromised state are predisposing factors.[2] Phlegmonous gastritis rarely develops after therapeutic endoscopy and only a few instances have been reported.[3] We describe a patient with PG that arose as a complication after endoscopic ultrasound-guided fine-needle aspiration (EUS-FNA).

A 70-year-old woman with a diagnosis of pancreatic tumor attended our hospital. A 50-mm, low echoic lesion at the pancreatic body was identified by EUS and EUS-FNA proceeded through the stomach using a 19-gauge needle (Echo Tip®Ultra; Wilson-Cook, Winston Salem, NC, USA). She was discharged on the following day. She returned to our hospital 1 week later due to persistent upper abdominal pain and low-grade fever. Her vital signs were: blood pressure, 105/66 mmHg; regular pulse, 96 b.p.m. and temperature of 38°C.

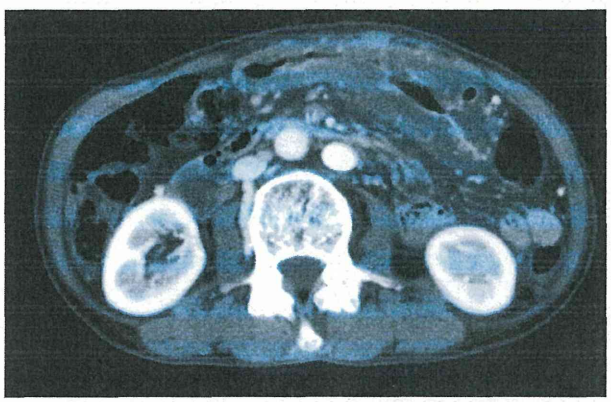

Fig. 1. Multi-detector computed tomography image. Air is trapped in diffusely thickened gastric wall.

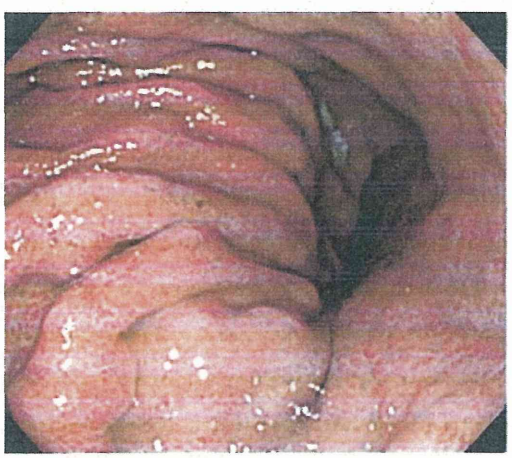

Fig. 2. Upper gastrointestinal endoscopy shows diffuse erythema, edema and erosions.

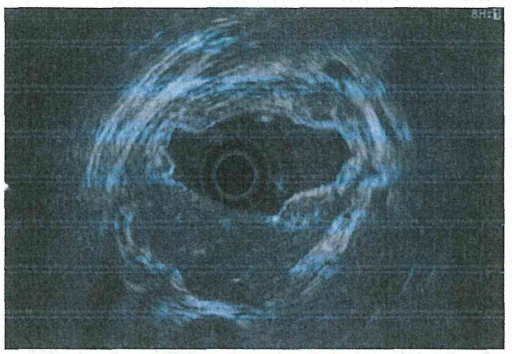

Fig. 3. Endoscopic ultrasound shows submucosa of gastric wall is predominantly thickened.

The patient's abdomen was soft, flat, and slightly distended with mild tenderness in the upper area. The laboratory findings were as follows: obvious inflammation with white blood cells (WBC) 13 500/μL and C-reactive protein (CRP) 28 mg/dL. Multi-detector row computed tomography (MDCT) revealed diffuse thickening of the gastric wall and air trapped within it (Fig. 1). Upper gastrointestinal endoscopy revealed diffuse erythema, edema and erosions (Fig. 2). EUS also showed diffuse gastric wall thickening, predominantly in the submucosa (Fig. 3). The culture of several biopsy specimens from the mucosal surface revealed *α-Streptococcus* and PG caused by EUS-FNA was clinically diagnosed. The patient recovered after antibiotic therapy with peperacillin/tazobactam and she was discharged on hospital day 15.

EUS-FNA is a safe procedure with a complication rate of approximately 1% that does not normally require antibiotic prophylaxis.[4] However, the risk of PG must be considered for immunocompromised patients with advanced cancer and preventative antibiotics may be necessary.

Masahiro Itonaga, Kazuki Ueda and Masao Ichinose
Second Department of Internal Medicine, Wakayama Medical University, Wakayama, Japan

REFERENCES

1. Soon MS, Yen HH, Soon A, Lin OS. Endoscopic ultrasonographic appearance of gastric emphysema. *World J. Gastroenterol.* 2005; **11**: 1719–21.
2. Park CW, Kim A, Cha SW *et al.* A case of phlegmonous gastritis associated with marked gastric distension. *Gut Liver* 2010; **4**: 415–18.
3. Lee BS, Kim SM, Seong JK *et al.* Phlegmonous gastritis after endoscopic mucosal resection. *Endoscopy* 2005; **37**: 490–3.
4. Polkowski M, Larghi A, Weynand B *et al.* Learning, techniques, and complications of endoscopic ultrasound (EUS)-guided sampling in gastroenterology: European Society of Gastrointestinal Endoscopy (ESGE) Technical Guideline. *Endoscopy* 2012; **44**: 190–206.

© 2012 The Authors
Digestive Endoscopy © 2012 Japan Gastroenterological Endoscopy Society

World Journal of Gastrointestinal Endoscopy

Online Submissions: http://www.wjgnet.com/1948-5190office
wjge@wjgnet.com
doi:10.4253/wjge.v4.i3.80

World J Gastrointest Endosc 2012 March 16; 4(3): 80-86
ISSN 1948-5190 (online)
© 2012 Baishideng. All rights reserved.

ORIGINAL ARTICLE

Diazepam during endoscopic submucosal dissection of gastric epithelial neoplasias

Yosuke Muraki, Shotaro Enomoto, Mikitaka Iguchi, Toru Niwa, Takao Maekita, Takeichi Yoshida, Kosaku Moribata, Naoki Shingaki, Hisanobu Deguchi, Kazuki Ueda, Izumi Inoue, Hideyuki Tamai, Jun Kato, Mitsuhiro Fujishiro, Masao Ichinose

Yosuke Muraki, Shotaro Enomoto, Mikitaka Iguchi, Toru Niwa, Takao Maekita, Takeichi Yoshida, Kosaku Moribata, Naoki Shingaki, Hisanobu Deguchi, Kazuki Ueda, Izumi Inoue, Hideyuki Tamai, Jun Kato, Masao Ichinose, Second Department of Internal Medicine, Wakayama Medical University, Wakayama City, Wakayama 641-0012, Japan
Mitsuhiro Fujishiro, Department of Endoscopy and Endoscopic Surgery, Faculty of Medicine, University of Tokyo, Bunkyo-ku, Tokyo 113-8655, Japan
Author contributions: Muraki Y drafted the manuscript; Enomoto S made preparations for this manuscript; Maekita T, Yoshida T, Moribata K, Shingaki N, Deguchi H, Ueda K, Inoue I, Tamai H and Kato J contributed to data acquisition; Iguchi M, Niwa T, Fujishiro M and Ichinose M contributed to the analysis, interpretation of the data and critical revision of the manuscript for important intellectual content. All of the authors approved the final manuscript.
Supported by A Grant-in-Aid for Cancer Research from the Ministry of Health, Labor and Welfare of Japan, in part
Correspondence to: Shotaro Enomoto, MD, PhD, Second Department of Internal Medicine, Wakayama Medical University, 811-1 Kimiidera, Wakayama City, Wakayama 641-0012, Japan. shoe@orion.ocn.ne.jp
Telephone: +81-73-447-1335 Fax: +81-73-445-3616
Received: September 7, 2011 Revised: January 17, 2012
Accepted: March 2, 2012
Published online: March 16, 2012

Abstract

AIM: To investigate risk factors and adverse events related to high-dose diazepam administration during endoscopic submucosal dissection for gastric neoplasias.

METHODS: Between February 2002 and December 2009, a total of 286 patients with gastric epithelial neoplasia underwent endoscopic submucosal dissection in our hospital. To achieve moderate sedation, 5-7.5 mg of diazepam was administered intravenously by non-anesthesiologists. Intermittent additional administration of 2.5-5 mg diazepam was performed if uncontrollable body movement of the patient was observed. All patients were classified into groups based on the required diazepam dose: low-dose ($\leq$ 17.5 mg, n = 252) and high-dose (> 17.5 mg, n = 79).

RESULTS: Differences between the low- and high-dose diazepam groups were observed in lifetime alcohol consumption (0.30 ± 0.48 *vs* 0.44 ± 0.52 tons, P = 0.032), body weight (58.4 ± 10.3 *vs* 62.0 ± 9.9 kg, P = 0.006), tumor size (15 ± 10 *vs* 23 ± 18 mm, P < 0.001), lesion location (P < 0.001) and the presence of ulcerative findings (14/238 *vs* 18/61, P < 0.001). Multivariate analysis identified all five variables as independently related to required diazepam dosage. In terms of adverse reactions to diazepam administration, paradoxical excitement was significantly more frequent in the high-dose diazepam group (P < 0.001).

CONCLUSION: Intermittent administration of diazepam enabled safe completion of gastric endoscopic submucosal dissection except in patients who were alcohol abusers or obese, or who showed complicated lesions.

© 2012 Baishideng. All rights reserved.

Key words: Diazepam; Endoscopic submucosal dissection; Gastric epithelial neoplasias; Moderate sedation; Non-anesthesiologists

Peer reviewers: Andreas Probst, MD, Department of Gastroenterology, Klinikum Augsburg, Stenglinstrasse 2, 86156 Augsburg, Germany; Hoon Jai Chun, Professor, Korea University College of Medicine, 126-1, 5-ga Anam-dong, Seongbuk-gu, Seoul 136-705, South Korea

Muraki Y, Enomoto S, Iguchi M, Niwa T, Maekita T, Yoshida T,

Moribata K, Shingaki N, Deguchi H, Ueda K, Inoue I, Tamai H, Kato J, Fujishiro M, Ichinose M. Diazepam during endoscopic submucosal dissection of gastric epithelial neoplasias. *World J Gastrointest Endosc* 2012; 4(3): 80-86 Available from: URL: http://www.wjgnet.com/1948-5190/full/v4/i3/80.htm DOI: http://dx.doi.org/10.4253/wjge.v4.i3.80

INTRODUCTION

Endoscopic submucosal dissection (ESD) is a novel and minimally invasive procedure for the treatment of gastric epithelial neoplasia. As this technique permits en bloc resection of lesions, ESD has the advantages of enabling accurate pathological assessment and reducing the risk of local recurrence[1]. However, in comparison to conventional endoscopic mucosal resection (EMR), ESD requires a high level of endoscopic competence and a longer resection time[2-4]. In addition, many cases of early gastric cancer occur in elderly patients, who also display increased sensitivity to sedatives and a higher risk of adverse reactions, including respiratory and cardiovascular depression[5]. Suitable sedatives that do not cause complications and permit safe completion of ESD thus need to be identified.

The American Society of Anesthesiologists (ASA) classifies the degree of sedation into four levels: minimal sedation; moderate or conscious sedation; deep sedation; and general anesthesia[6]. Given that deep sedation or even general anesthesia can be achieved with propofol, the ASA suggests that care must be taken even if aiming for moderate sedation[6]. In addition, due to the narrow therapeutic window[7-9], the American Society for Gastrointestinal Endoscopy has recommended the presence of trained personnel dedicated to the administration of propofol[10]. To date, the safety and efficacy of sedation using propofol have been reported in esophagogastroduodenoscopy, colonoscopy, endoscopic ultrasonography and endoscopic retrograde cholangiopancreatography[11-15]. In contrast, due to the risk of cardiorespiratory complications, particularly in the elderly, the Japan Gastroenterological Endoscopy Society does not recommend sedation using propofol for endoscopic procedures. Thus, there is an in-principle requirement in Japan that propofol be administered by an anesthesiologist. As a result, not many institutions use propofol for sedation during ESD[16,17].

Of the available sedatives, benzodiazepines are generally considered to have a broad safety margin as they do not activate the gamma-aminobutyric acid $(GABA)_A$ receptor in the absence of endogenous GABA[18]. Diazepam is the least potent injectable benzodiazepine sedative, with a long history of clinical use, even by non-anesthesiologists. Moreover, unlike in the case of propofol administration, if a patient falls into deep sedation while being treated with diazepam, a pharmacological antagonist (flumazenil) can be administered to counter this effect[19,20]. Fujishiro *et al*[21] reported that, in principle, ESD for esophageal squamous cell neoplasms could be performed with the patient under conscious sedation induced by intermittent administration of diazepam and pentazocine. However, administration methods have yet to be clearly established for safe and effective sedative use during the gastric ESD procedure.

The objectives in this retrospective study were to evaluate variables relating to the diazepam dosage during ESD for gastric epithelial neoplasia and to investigate the characteristics and adverse events of patients administered high-dose diazepam.

MATERIALS AND METHODS

Patients

Between February 2002 and December 2009, we performed ESD for 446 gastric epithelial neoplastic lesions in 342 consecutive patients treated at Wakayama Medical University Hospital. ESD was indicated for patients with adenomas suspected of being malignant on the basis of endoscopic findings or biopsy. In addition, ESD was indicated for patients with early gastric cancers that were considered to have a nominal risk of lymph node metastasis according to the criteria of Gotoda *et al*[22], excluding undifferentiated cancers. For this study, we retrospectively analyzed ESDs that had been performed for 331 lesions in 286 patients (mean age, 69.5 years; range, 42-90 years). Excluded lesions comprised 77 cases for which multiple lesions had been simultaneously dissected by ESD, 26 cases for which diazepam had not been administered, 7 lesions in which other investigations had been carried out, and 7 lesions for which the intraoperative records were unclear (with an overlap of 2 lesions). All patients underwent blood tests, chest X-rays and electrocardiographic testing before treatment. ESD was indicated for patients with an ASA classification of 1-3[23]. This study was approved by the ethics committee of Wakayama Medical University, and all patients provided written informed consent prior to undergoing ESD.

ESD procedures

ESD was performed by one of four experienced therapeutic endoscopists, each of whom had performed ESD for more than 50 cases of early gastric cancer or gastric adenoma. We predominantly used a flex electrosurgical knife (KD-630L; Olympus, Tokyo, Japan)[2,24], along with a hook knife (KD-620LR; Olympus) when necessary[25]. Hemostatic forceps (HDB2422W; Pentax, Tokyo, Japan)[26-28] were used to reduce bleeding during ESD.

Diazepam administration

We aimed to achieve moderate sedation during ESD. For introduction, we intravenously administered diazepam (Cercine®; Takeda Pharmaceutical, Osaka, Japan) at 5-7.5 mg/body (5 mg/body for patients $\geq$ 75 years old or weighing $\leq$ 50 kg) prior to insertion of the endoscope; in principle, administration of diazepam was continued

up to 10 mg during ESD. When the sedative effect of 10 mg diazepam was judged sufficient, administration of the drug was continued without any change, and additional administration was performed in intermittent doses of 2.5-5 mg/body each, only when uncontrollable body movement was observed (maximal dose: 40 mg). When the sedative effect of 10 mg diazepam was judged to be insufficient and patient distress was considered great, diazepam was switched to midazolam (Dormicum®; Astellas Pharmaceutical, Tokyo, Japan) for rescue, administered intermittently at 1-2 mg/body. Intermittent sedative administration was performed by non-anesthesiologists (i.e., gastroenterologists) at the direction of the operator. For the purposes of pain relief, 15 mg of pentazocine (Sosegon®; Astellas Pharmaceutical) was administered intramuscularly to all patients at the start of ESD. When the level of anesthesia reached deep sedation, flumazenil (Anexate®; Astellas Pharmaceutical) was administered as deemed necessary.

Patient monitoring

Blood pressure, heart rate, electrocardiography (ECG), and peripheral oxygen saturation (SpO_2) were monitored during the procedure. Blood pressure was measured at 5-min intervals, while heart rate, ECG tracing and SpO_2 were measured continuously. Supplementary oxygen was administered to patients with SpO_2 below 90%. Administered dosages of sedatives and analgesics, all adverse events (such as decreases in SpO_2 below 90% and blood pressure below 90 mmHg), and uncontrollable body movements were recorded by trained nurses.

Patients were instructed to rest in bed for 3 h following ESD, and to remain under strict observation until the next morning. All ESD procedures were performed on an inpatient basis, and patients were discharged within 10 days after ESD if no problems were encountered.

Parameters assessed

Since several reports have indicated that it is advisable that ESD requiring around 1.5 h or more should be carried out under general anesthesia[21], patients were stratified into two groups according to procedure time ($\leqslant$ 1.5 h or > 1.5 h) and then compared in terms of the following variables: age; sex; lifetime alcohol consumption; smoking habit; body weight (BW); tumor size (maximal diameter of the lesion); location (upper-third, middle-third, or lower-third of the stomach); gross morphological type (0-Ⅰ/Ⅱa, 0-Ⅱb/Ⅱc or combined type); tumor depth (mucosal or submucosal tumor); histological type (cancer or adenoma); ulcerative findings in the submucosal layer; and diazepam dosage.

Patients were also stratified into two groups according to diazepam dose: low-dose diazepam ($\leqslant$ 17.5 mg, n = 252) and high-dose diazepam (> 17.5 mg, n = 79). These two groups were then compared in terms of age, sex, lifetime alcohol consumption, smoking habit, BW, use of anxiolytic agents, ASA classification, comorbidities (hypertension, diabetes mellitus, heart disease, respiratory disease, chronic renal failure, or liver cirrhosis), tumor size, tumor location, gross morphological type, tumor depth, histological type, ulcerative findings, type of resection (en bloc or piecemeal), postoperative bleeding, perforation, use of midazolam, and sedative-related adverse events such as oxygen desaturation (SpO_2 below 90%), hypotension (blood pressure below 90 mmHg), delayed awakening and paradoxical excitement.

Statistical analysis

Univariate analysis was performed using an unpaired t-test for numerical data and Fisher's exact test or the chi-squared test for categorical data. Variables that differed significantly between groups in univariate analysis were then subjected to multivariate analysis using a logistic regression model. All tests were two-sided, with values of $P < 0.05$ being considered statistically significant. All analyses were performed using SPSS software (SPSS, Chicago, IL, United States).

RESULTS

Comparison of clinicopathological features according to procedure time

The outcome of univariate analyses comparing variables according to the ESD procedure time (i.e., $\leqslant$ 1.5 h *vs* > 1.5 h) is outlined in Table 1. Significant differences were found between the two groups in relation to tumor size, location, ulcerative findings and diazepam dosage ($P <$ 0.001, respectively). Specifically, mean diazepam dosage among patients with an ESD procedure time of > 1.5 h was 17.5 mg.

Comparison of clinicopathological features according to diazepam dose

Based on the above results, patients were divided into a low-dose ($\leqslant$ 17.5 mg) diazepam group and a high-dose (> 17.5 mg) diazepam group. Results of univariate analyses of patient variables in relation to diazepam dosage are shown in Table 2. Significant differences in lifetime alcohol consumption and BW (P = 0.032 and P = 0.006, respectively) were found between the dosage groups. The results of univariate analyses for clinicopathological features of the lesion and clinical outcomes in relation to diazepam dosage are shown in Table 3. Significant differences in tumor size, location, ulcerative findings and resection style (P = 0.001 for each) were found between the two dosage groups.

Multivariate logistic analysis was performed including lifetime alcohol consumption, BW, tumor size, location and ulcerative findings in the prediction of the diazepam dosage. Each variable included in the model was shown to be independently associated with a need for high diazepam dosage (Table 4).

Patients were stratified into two groups on the basis of lifetime alcohol consumption (alcohol), using > 0.4 and $\leqslant$ 0.4 t as the strata. Finally, a second stratification was performed on the basis of BWs of > 60 kg and $\leqslant$

Table 1 Clinicopathological features of study subjects with a low (≤ 1.5 h) or high (> 1.5 h) procedure time

Variables	Procedure time ≤ 1.5 h (n = 180)	Procedure time > 1.5 h (n = 151)	P value
Age (yr) (mean ± SD)	69.9 ± 9.1	69.0 ± 9.6	NS
Sex (male/female)	136/44	125/26	NS
Lifetime alcohol consumption (t) (mean ± SD)	0.30 ± 0.50	0.37 ± 0.48	NS
Smoking habit (Brinkman index) (mean ± SD)	655.1 ± 777.7	563.0 ± 666.9	NS
Body weight (kg) (mean ± SD)	58.5 ± 10.9	60.1 ± 9.6	NS
Tumor size (mm) (mean ± SD)	13.3 ± 7.7	22.3 ± 16.0	< 0.001
Tumor location in stomach (U + M/L)	54/126	94/57	< 0.001
Gross morphological type (0-I / IIa *vs* 0-IIb / IIc *vs* combined)	92/68/20	76/66/9	NS
Tumor depth (mucosa/submucosa)	168/12	134/17	NS
Histological type (cancer/adenoma)	124/56	108/43	NS
Ulcerative findings, n (%)	2 (1.1)	30 (19.9)	< 0.001
Diazepam (mg) (mean ± SD)	9.9 ± 3.3	17.5 ± 7.8	< 0.001

SD: Standard deviation; NS: Not significant; U: Upper-third of the stomach; M: Middle-third of the stomach; L: Lower-third of the stomach.

Table 2 Clinical features of study subjects administered low- or high-dose of diazepam

Variables	Low-dose group (n = 252)	High-dose group (n = 79)	P value
Age (yr) (mean ± SD)	69.8 ± 9.1	68.3 ± 10.1	NS
Sex (male / female)	194/58	67/12	NS
Lifetime alcohol consumption (t) (mean ± SD)	0.30 ± 0.48	0.44 ± 0.52	0.032
Smoking habit (Brinkman index) (mean ± SD)	649.5 ± 767.7	497.8 ± 582.5	NS
Body weight (kg) (mean ± SD)	58.4 ± 10.3	62.0 ± 9.9	0.006
Anxiolytic agents (used/not used)	46/206	7/72	NS
ASA classification (ASA 1/ASA 2 / ASA 3)	48/151/53	20/47/12	NS
Comorbidities			
Hypertension, n (%)	127 (50.3)	39 (49.4)	NS
Diabetes mellitus, n (%)	44 (17.5)	11 (13.9)	NS
Heart disease, n (%)	58 (23.0)	18 (22.8)	NS
Respiratory disease, n (%)	30 (11.9)	4 (5.1)	NS
Chronic renal failure, n (%)	4 (1.6)	0 (0)	NS
Liver cirrhosis, n (%)	21 (8.3)	5 (6.3)	NS

SD: Standard deviation; NS: Not significant; ASA: American Society of Anesthesiologists.

60 kg. Thus, four subgroups were created and analyzed in relation to the diazepam dosage. The odds ratios of this logistic regression analysis are shown in Table 5. The combination of alcohol ≤ 0.4 t and BW ≤ 60 kg was defined as the standard subgroup. Odds ratios for

Table 3 Clinicopathological features and clinical outcomes of subjects administered low- or high-dose of diazepam

Variables	Low-dose group (n = 252)	High-dose group (n = 79)	P value
Tumor size (mm) (mean ± SD)	15.4 ± 10.1	23.9 ± 18.2	< 0.001
Tumor location in stomach (U and M/L)	96/156	52/27	< 0.001
Gross morphological type (0-I / IIa *vs* 0-IIb / IIc *vs* combined)	129/100/23	39/34/6	NS
Tumor depth (mucosa/submucosa)	233/19	69/10	NS
Histological type (cancer/ adenoma)	176/76	56/23	NS
Ulcerative findings, n (%)	14 (5.6)	18 (22.8)	< 0.001
Resection style (en bloc/piecemeal)	246/6	63/16	< 0.001
Postoperative bleeding, n (%)	1 (0.4)	1 (1.3)	NS
Perforation, n (%)	8 (3.2)	6 (7.6)	NS
Midazolam (added / not added)	43/209	20/59	NS

SD: Standard deviation; NS: Not significant; U: Upper-third of the stomach; M: Middle-third of the stomach; L: Lower-third of the stomach.

Table 4 Factors associated with the need for high doses of diazepam: Results of multivariate logistic analysis

Variable	P value	Odds ratio	95% CI
Lifetime alcohol consumption	0.041	1.74	1.02-2.97
Body weight	0.034	1.03	1.00-1.06
Tumor size	0	1.05	1.03-1.08
Location in stomach	0	2.87	1.61-5.12
Ulcerative findings	0.001	4.45	1.92-10.34

CI: Confidence interval.

the other three subgroups were found to increase in a stepwise fashion, with the greatest risk of high diazepam dose among patients with both alcohol > 0.4 t and BW > 60 kg (odds ratio = 4.52, 95% CI: 2.07 to 9.86).

Adverse events

Comparisons of adverse events according to diazepam dosage are included in Table 6. The incidence of paradoxical excitement was significantly higher in the high-dose diazepam group (P < 0.001). However, no other significant differences in adverse events were found.

DISCUSSION

This retrospective study revealed that gastric ESD can be performed in nearly 80% of patients under sedation achieved using a low dosage of diazepam. Patients with a long ESD procedure time were characterized by large-diameter tumors, lesions located in the upper- or middle-third of the stomach, and those accompanied by ulcerative findings. Outcomes found to be predictive of

Table 5 Comparison of need for high diazepam dose between subgroups stratified for lifetime alcohol consumption and body weight

Subgroup	Low-dose group (n = 252)	High-dose group (n = 79)	Odds ratio	95% CI
Alcohol > 0.4 t, BW > 60 kg	31	20	4.52	2.07-9.86
Alcohol > 0.4 t, BW ≤ 60 kg	38	17	3.13	1.43-6.88
Alcohol ≤ 0.4 t, BW > 60 kg	72	27	2.63	1.31-5.28
Alcohol ≤ 0.4 t, BW ≤ 60 kg	105	15	1	Referent

CI: Confidence interval. Alcohol: Lifetime alcohol consumption; BW: Body weight.

Table 6 Adverse events in patients administered a low *vs* high dose of diazepam

Variables	Low-dose group (n = 252)	High-dose group (n = 79)	P value
SpO2 < 90%, n (%)	70 (27.8)	18 (22.8)	NS
Blood pressure < 90 mmHg, n (%)	8 (3.2)	2 (2.5)	NS
Delayed awakening (flumazenil used/not used)	4/248	0/79	NS
Paradoxical excitement, n (%)	6 (2.4)	13 (16.5)	< 0.001

NS: Not significant.

a long ESD procedure time in the current study agreed with those previously reported by Goto *et al*[29]. To the best of our knowledge, no previous reports have confirmed that the sedative dose used during gastric ESD is increased in special patient groups (e.g., alcoholics or patients with higher BW). However, we found that a number of lesion-specific findings, as well as lifetime alcohol consumption and BW, were also associated with high-dose diazepam administration. In particular, lifetime alcohol consumption > 0.4 t and BW > 60 kg were additive risk factors for increased diazepam dosage. Specifically, patients with both a lifetime alcohol consumption > 0.4 t and a BW > 60 kg showed the greatest risk of needing a high diazepam dosage during ESD. While habitual alcohol consumption may increase the clearance of diazepam, the high lipid-solubility of diazepam may also result in rapid removal from the plasma and uptake by adipose tissue[30,31]. Therefore, when predicting diazepam dosages prior to starting gastric ESD, it is important to take into account not only the difficulty of the ESD procedure, but also the alcohol history and BW of the patient.

Although both respiratory and cardiovascular depression are common adverse events of diazepam administration, we encountered no serious events in the current study. For example, while oxygen saturation < 90% was observed in approximately 26% of patients, all recovered quickly in response to intraoperative supplemental oxygen administration and none required endotracheal intubation.

Debate is continuing regarding the proper depth of anesthesia required to perform lengthy endoscopic procedures such as ESD. We consider moderate sedation, which does not appear to cause respiratory depression, as the appropriate level of sedation. If the aim is to maintain the patient under moderate sedation with intermittent administration of a benzodiazepine, long-acting drugs such as diazepam are thought to be suitable in treatments requiring a relatively long time. Indeed, ESD procedures in almost all Japanese institutions are performed by an endoscopist who not only performs the ESD, but is also responsible for sedation during the operation. Due to a long half-life, diazepam is more suitable for intermittent than for continuous administration. Furthermore, intermittent administration in response to uncontrollable body movement is easy for a single operator to manage. The current analysis did not find any significant differences in the incidence of oxygen desaturation (SpO_2 below 90%) or hypotension (blood pressure below 90 mmHg) as a function of the administered diazepam dosage. These findings not only indicate the safety of diazepam, but also the suitability of its administration method.

Due to deep sedation in response to diazepam in the low-dosage diazepam group, flumazenil had to be administered to 4 patients (1.2%). Three of those patients had been coadministered 10 mg of midazolam, while another was an 85-year-old patient with a BW of only 42 kg. Kiriyama *et al*[17] reported that post-ESD recovery from sedation was faster with propofol than with midazolam. The present study did not perform scoring to investigate the recovery from sedation, but almost all patients were awake after returning to their hospital room following completion of the ESD procedure. Also, no cases showed carry-over of the sedative effect to the following morning. All patients who were administered flumazenil also showed rapid awakening, and no problems due to re-sedation were noted. Nevertheless, since ESD in Japan is currently performed as an inpatient treatment, as long as sufficient postoperative management is carried out, there may be no need for quick recovery of wakefulness.

Paradoxical excitement represents restless motion that occurs during diazepam administration. This reaction is reportedly caused, at least in part, by the toxicity of propylene glycol, an included diazepam solvent[32]. Propylene glycol is also a solvent that causes local irritation of veins. Some patients in the present study complained of transient vascular pain, but phlebitis was not seen in any patients. However, a notable increase in restlessness was observed with increasing diazepam dosages. Such reactions made the operation difficult to continue. Accordingly, in cases where preoperative prediction shows a strong possibility that a large dose of diazepam will be required, a different approach to sedation may be advisable. Examples include continuously administering propofol or dexmedetomidine from the start of the

operation, a technique that has recently been reported as useful during ESD[17,33].

The present study has several limitations. First, data generated from only a single hospital were reviewed retrospectively. Second, the decision to administer additional diazepam was left up to the operator, and the timing of such administration was not consistent across patients. However, the most important aspect of this study was the evaluation of the suitability of intermittent administration of diazepam prior to ESD. Further studies at multiple institutions should be conducted using different benzodiazepines and concomitant drugs, with different methods of administration.

In conclusion, among patients who are predicted to require only a low dosage of diazepam during ESD, intermittent administration of diazepam for sedation during gastric ESD will enable safe completion of the surgery. The need for high-dose diazepam can be expected in patients with lifetime alcohol consumption > 0.4 t, BW > 60 kg, or requiring a technically difficult ESD procedure. Given the present results, further randomized trials performed in a prospective manner with clear inclusion criteria and a clear injection protocol should be conducted for such patients.

ACKNOWLEDGMENTS

We would like to express our deepest thanks to Ms. Kazu Konishi for her excellent secretarial assistance.

COMMENTS

Background

Endoscopic submucosal dissection (ESD) is a curative treatment for gastric epithelial neoplasia. Many cases of gastric epithelial neoplasia occur in elderly patients, who show increased sensitivity to sedatives and a higher risk of adverse reactions. Suitable methods for the administration of sedatives during ESD thus need to be established.

Research frontiers

This study can help us to understand the diazepam dosage required during ESD for gastric epithelial neoplasia and the characteristics of and adverse events encountered by patients administered high-dose diazepam.

Innovations and breakthroughs

Diazepam is the least potent injectable benzodiazepine sedative, with a long history of clinical use. However, administration methods have yet to be clearly established for safe and effective sedative use during gastric ESD procedures.

Applications

The results have demonstrated that intermittent administration of diazepam enabled safe completion of gastric ESD except for patients who are alcohol abusers or obese, or those with complicated lesions.

Peer review

This retrospective study investigated risk factors and adverse events related to high-dose diazepam administration during ESD for gastric neoplasias. Based on the present results, further randomized trials performed prospectively with clear inclusion criteria and a clear injection protocol should be conducted.

REFERENCES

1 **Kakushima N**, Fujishiro M. Endoscopic submucosal dissection for gastrointestinal neoplasms. *World J Gastroenterol* 2008; **14**: 2962-2967
2 **Yahagi N**, Fujishiro M, Kakushima N, Kobayashi K, Hashimoto T, Oka M, Iguchi M, Enomoto S, Ichinose M, Niwa H, Omata M. Endoscopic submucosal dissection for early gastric cancer using the tip of an electrosurgical snare (thin type). *Dig Endosc* 2004; **16**: 34-38
3 **Oda I**, Gotoda T, Hamanaka H, Takako E, Yutaka S, Matsuda T, Bhandari P, Emura F, Saito D, Ono H. Endoscopic submucosal dissection for early gastric cancer: technical feasibility, operation time and complications from a large consecutive series. *Dig Endosc* 2005; **17**: 54-58
4 **Fujishiro M**. Endoscopic submucosal dissection for stomach neoplasms. *World J Gastroenterol* 2006; **12**: 5108-5112
5 **Kakushima N**, Fujishiro M, Kodashima S, Muraki Y, Tateishi A, Yahagi N, Omata M. Technical feasibility of endoscopic submucosal dissection for gastric neoplasms in the elderly Japanese population. *J Gastroenterol Hepatol* 2007; **22**: 311-314
6 Practice guidelines for sedation and analgesia by non-anesthesiologists. *Anesthesiology* 2002; **96**: 1004-1017
7 **Carlsson U**, Grattidge P. Sedation for upper gastrointestinal endoscopy: a comparative study of propofol and midazolam. *Endoscopy* 1995; **27**: 240-243
8 **Schnider TW**, Minto CF, Shafer SL, Gambus PL, Andresen C, Goodale DB, Youngs EJ. The influence of age on propofol pharmacodynamics. *Anesthesiology* 1999; **90**: 1502-1516
9 **Tohda G**, Higashi S, Wakahara S, Morikawa M, Sakumoto H, Kane T. Propofol sedation during endoscopic procedures: safe and effective administration by registered nurses supervised by endoscopists. *Endoscopy* 2006; **38**: 360-367
10 **Faigel DO**, Baron TH, Goldstein JL, Hirota WK, Jacobson BC, Johanson JF, Leighton JA, Mallery JS, Peterson KA, Waring JP, Fanelli RD, Wheeler-Harbaugh J. Guidelines for the use of deep sedation and anesthesia for GI endoscopy. *Gastrointest Endosc* 2002; **56**: 613-617
11 **Koshy G**, Nair S, Norkus EP, Hertan HI, Pitchumoni CS. Propofol versus midazolam and meperidine for conscious sedation in GI endoscopy. *Am J Gastroenterol* 2000; **95**: 1476-1479
12 **Vargo JJ**, Zuccaro G, Dumot JA, Shermock KM, Morrow JB, Conwell DL, Trolli PA, Maurer WG. Gastroenterologist-administered propofol versus meperidine and midazolam for advanced upper endoscopy: a prospective, randomized trial. *Gastroenterology* 2002; **123**: 8-16
13 **Yusoff IF**, Raymond G, Sahai AV. Endoscopist administered propofol for upper-GI EUS is safe and effective: a prospective study in 500 patients. *Gastrointest Endosc* 2004; **60**: 356-360
14 **Wehrmann T**, Kokabpick S, Lembcke B, Caspary WF, Seifert H. Efficacy and safety of intravenous propofol sedation during routine ERCP: a prospective, controlled study. *Gastrointest Endosc* 1999; **49**: 677-683
15 **Jung M**, Hofmann C, Kiesslich R, Brackertz A. Improved sedation in diagnostic and therapeutic ERCP: propofol is an alternative to midazolam. *Endoscopy* 2000; **32**: 233-238
16 **Imagawa A**, Fujiki S, Kawahara Y, Matsushita H, Ota S, Tomoda T, Morito Y, Sakakihara I, Fujimoto T, Taira A, Tsugeno H, Kawano S, Yagi S, Takenaka R. Satisfaction with bispectral index monitoring of propofol-mediated sedation during endoscopic submucosal dissection: a prospective, randomized study. *Endoscopy* 2008; **40**: 905-909
17 **Kiriyama S**, Gotoda T, Sano H, Oda I, Nishimoto F, Hirashima T, Kusano C, Kuwano H. Safe and effective sedation in endoscopic submucosal dissection for early gastric cancer: a randomized comparison between propofol continuous infusion and intermittent midazolam injection. *J Gastroenterol* 2010; **45**: 831-837
18 **Mendelson WB**. Neuropharmacology of sleep induction by benzodiazepines. *Crit Rev Neurobiol* 1992; **6**: 221-232
19 **Haefely W**. The preclinical pharmacology of flumazenil. *Eur J Anaesthesiol Suppl* 1988; **2**: 25-36
20 **Mould DR**, DeFeo TM, Reele S, Milla G, Limjuco R, Crews

T, Choma N, Patel IH. Simultaneous modeling of the pharmacokinetics and pharmacodynamics of midazolam and diazepam. *Clin Pharmacol Ther* 1995; **58**: 35-43

21 **Fujishiro M**, Kodashima S, Goto O, Ono S, Niimi K, Yamamichi N, Oka M, Ichinose M, Omata M. Endoscopic submucosal dissection for esophageal squamous cell neoplasms. *Dig Endosc* 2009; **21**: 109-115

22 **Gotoda T**, Yanagisawa A, Sasako M, Ono H, Nakanishi Y, Shimoda T, Kato Y. Incidence of lymph node metastasis from early gastric cancer: estimation with a large number of cases at two large centers. *Gastric Cancer* 2000; **3**: 219-225

23 **Lichtenstein DR**, Jagannath S, Baron TH, Anderson MA, Banerjee S, Dominitz JA, Fanelli RD, Gan SI, Harrison ME, Ikenberry SO, Shen B, Stewart L, Khan K, Vargo JJ. Sedation and anesthesia in GI endoscopy. *Gastrointest Endosc* 2008; **68**: 205-216

24 **Kodashima S**, Fujishiro M, Yahagi N, Kakushima N, Omata M. Endoscopic submucosal dissection using flexknife. *J Clin Gastroenterol* 2006; **40**: 378-384

25 **Oyama T**, Kikuchi Y. Aggressive endoscopic mucosal resection in the upper GI tract-hook knife EMR method. *Minim Invasive Ther Allied Technol* 2002; **11**: 291-295

26 **Enomoto S**, Yahagi N, Fujishiro M, Oka M, Kakushima N, Iguchi M, Yanaoka K, Arii K, Tamai H, Shimizu Y, Omata M, Ichinose M. Novel endoscopic hemostasis technique for use during endoscopic submucosal dissection. *Endoscopy* 2007; **39** Suppl 1: E156

27 **Enomoto S**, Yahagi N, Fujishiro M, Iguchi M, Ichinose M. Endoscopic hemostasis using high-frequency hemostatic forceps for hemorrhagic gastric ulcer. *Nihon Rinsho* 2004; **62**: 513-518

28 **Enomoto S**, Yahagi N, Fujishiro M, Oka M, Muraki Y, Deguchi H, Ueda K, Inoue I, Maekita T, Magari H, Mukoubayashi C, Nakazawa K, Iguchi M, Yanaoka K, Arii K, Tamai H, Omata M, Ichinose M. Assessment of intraoperative bleeding during endoscopic submucosal dissection and endoscopic hemostasis using high-frequency hemostatic forceps. *J Wakayama Med* 2009; **60**: 124-129

29 **Goto O**, Fujishiro M, Kodashima S, Ono S, Omata M. Is it possible to predict the procedural time of endoscopic submucosal dissection for early gastric cancer? *J Gastroenterol Hepatol* 2009; **24**: 379-383

30 **Kassai A**, Toth G, Eichelbaum M, Klotz U. No evidence of a genetic polymorphism in the oxidative metabolism of midazolam. *Clin Pharmacokinet* 1988; **15**: 319-325

31 **Persson MP**, Nilsson A, Hartvig P. Relation of sedation and amnesia to plasma concentrations of midazolam in surgical patients. *Clin Pharmacol Ther* 1988; **43**: 324-331

32 **Wilson KC**, Reardon C, Farber HW. Propylene glycol toxicity in a patient receiving intravenous diazepam. *N Engl J Med* 2000; **343**: 815

33 **Takimoto K**, Ueda T, Shimamoto F, Kojima Y, Fujinaga Y, Kashiwa A, Yamauchi H, Matsuyama K, Toyonaga T, Yoshikawa T. Sedation with dexmedetomidine hydrochloride during endoscopic submucosal dissection of gastric cancer. *Dig Endosc* 2011; **23**: 176-181

S- Editor Yang XC **L- Editor** Webster JR **E- Editor** Yang XC

Gastric Cancer (2012) 15:382–388
DOI 10.1007/s10120-011-0126-1

ORIGINAL ARTICLE

Identification of gastric cancer risk markers that are informative in individuals with past *H. pylori* infection

Sohachi Nanjo · Kiyoshi Asada · Satoshi Yamashita · Takeshi Nakajima · Kazuyuki Nakazawa · Takao Maekita · Masao Ichinose · Toshiro Sugiyama · Toshikazu Ushijima

Received: 25 August 2011 / Accepted: 26 November 2011 / Published online: 12 January 2012
© The International Gastric Cancer Association and The Japanese Gastric Cancer Association 2011

Abstract

Background Epigenomic damage induced by *Helicobacter pylori* infection is accumulated in gastric mucosae before the development of malignancy. In individuals without current *H. pylori* infection, DNA methylation levels of specific CpG islands (CGIs) are associated with gastric cancer risk. Because risk estimation in individuals with past infection is clinically important, we here aimed to identify the risk markers that reflect epigenomic damage induced by *H. pylori* infection, and that are informative in these individuals.

Methods Gastric mucosae were obtained from 55 gastric cancer patients (GC-Pt) (21 with current infection and 34 with past infection) and 55 healthy volunteers (HV) (7 never-infected, 21 with current infection, and 27 with past infection). Hypermethylated CGIs were searched for by methylated DNA immunoprecipitation-CGI microarray, and methylation levels were analyzed by quantitative methylation-specific polymerase chain reaction (PCR).

Results By microarray analysis of a pool of three samples from GC-Pt with past infection and another pool of samples from HV with past infection, 15 hypermethylated CGIs in the former pool were isolated. Seven of them had significantly higher methylation levels in GC-Pt with past infection ($n = 10$) than in HV with past infection ($n = 10$) ($P < 0.001$). In a validation cohort (21 GC-Pt with past infection and 14 HV with past infection), the seven new markers had large areas under the receiver-operating characteristic curves (0.78–0.84) and high odds ratios (12.7–36.0) compared with two currently available markers (0.60–0.65, 5.0–5.7).

Conclusions We identified seven novel gastric cancer risk markers that are highly informative in individuals with past infection.

Keywords Carcinogenesis · DNA methylation · Gastric cancer · *Helicobacter pylori*

Electronic supplementary material The online version of this article (doi:10.1007/s10120-011-0126-1) contains supplementary material, which is available to authorized users.

S. Nanjo · K. Asada · S. Yamashita · T. Ushijima (✉)
Division of Epigenomics, National Cancer Center Research Institute, 5-1-1 Tsukiji, Chuo-ku, Tokyo 104-0045, Japan
e-mail: tushijim@ncc.go.jp

S. Nanjo · T. Sugiyama
Third Department of Internal Medicine, University of Toyama, Toyama, Japan

T. Nakajima
Gastrointestinal Endoscopy Division, National Cancer Center Hospital, Tokyo, Japan

K. Nakazawa · T. Maekita · M. Ichinose
Second Department of Internal Medicine, Wakayama Medical University, Wakayama, Japan

Introduction

Early detection of cancer is critically important to reduce its morbidity and mortality, and early detection can be achieved by identifying individuals at high risk of developing cancers. In the risk estimation of gastric cancers, a history of *Helicobacter pylori* infection, which increases gastric cancer risk 2.2- to 21-fold [1–4], plays the major role, but the vast majority of individuals with a history of *H. pylori* infection do not develop gastric cancers. Also, gene polymorphisms associated with gastric cancers have been identified, and they have been shown to confer odds ratios (ORs) mostly between 1.0 and 2.0 [5, 6]. To obtain

clinically useful risk markers, we have to develop markers that are informative even in individuals with a history of *H. pylori* infection and that confer higher ORs.

Recently, we showed that *H. pylori* infection induces epigenomic damage, especially aberrant DNA methylation, in gastric mucosae [7]. DNA methylation levels of specific CpG islands (CGIs) were very high in the gastric mucosae of individuals with active *H. pylori* infection irrespective of gastric cancer risk, and decreased to certain levels after *H. pylori* was eradicated [8]. Importantly, these methylation levels in individuals without active *H. pylori* infection were correlated with gastric cancer risk [7, 9]. It is considered that aberrant DNA methylation is induced both in gastric stem cells and in non-stem cells, that methylation induced in stem cells will remain even after *H. pylori* eradication, and that methylation levels in individuals without current *H. pylori* infection reflect gastric cancer risk (degree of the epigenetic field defect) [10].

The correlation between methylation levels and gastric cancer risk has been analyzed in individuals without current *H. pylori* infection [7, 9]. Based on the data in our previous study [7], currently available methylation risk markers, *FLNc* and *THBD*, have ORs of 4.2–7.0 to detect gastric cancer patients (GC-Pt) among such individuals. However, individuals without current *H. pylori* infection indeed consist of never-infected individuals and those with past infection, and risk estimation is important in individuals with past infection.

In this study, we aimed to identify gastric cancer risk markers that reflect epigenomic damage induced by *H. pylori* infection, and that are informative in individuals with past infection.

Materials and methods

Tissue samples and determination of *H. pylori* infection status

Fifty-five healthy volunteers (HV) with endoscopic findings of no malignancy were recruited, with written informed consents, on the occasion of a gastric cancer screening program, with the approval of the institutional review board. Fifty-five GC-Pt who had undergone curative endoscopic submucosal dissection (ESD) of a well-differentiated adenocarcinoma in the non-cardia according to the Japanese classification of gastric carcinoma [11] were also recruited, with written informed consents, with the approval of the Institutional Review Board. Gastric mucosae were collected by endoscopic biopsy of the antrum. The biopsy specimens were frozen in liquid nitrogen immediately after biopsy, and stored at −80°C until DNA extraction. High molecular weight DNA was extracted by the phenol/chloroform method.

Current *H. pylori* infection was analyzed by a serum anti-*H. pylori* IgG antibody test (SRL, Tokyo, Japan) in HV and by urea breath test (Otsuka Pharmaceutical, Tokushima, Japan) in GC-Pt. Also, the presence of current or past *H. pylori* infection was detected by the endoscopic presence of atrophic gastritis in the antrum, because atrophic change induced by *H. pylori* infection arises in the antrum in 83% of individuals with *H. pylori* infection [12] and remains in all individuals who have had *H. pylori* eradication therapy [13]. "Never-infected individuals" were defined as those who were negative for *H. pylori* analysis and did not have atrophic gastritis in the antrum. "Individuals with current infection" were defined as those who were positive for *H. pylori* analysis. "Individuals with past infection" were defined as those who were negative for *H. pylori* analysis and had atrophic gastritis in the antrum.

Methylated DNA immunoprecipitation-CGI microarray analysis

Methylated DNA immunoprecipitation (MeDIP)-CGI microarray analysis was performed as previously described [14, 15]. Briefly, 5 μg of genomic DNA was immunoprecipitated with an anti-5-methylcytidine antibody (Diagnode, Liége, Belgium), and the precipitated DNA and the input DNA were labeled with cyanin (Cy) 5 and Cy3, respectively. A human CGI oligonucleotide microarray (Agilent Technologies, Santa Clara, CA, USA) was hybridized with the labeled probes and scanned with an Agilent G2565BA microarray scanner (Agilent Technologies). Scanned data were processed with Feature Extraction Software Version 9.1 (Agilent Technology) and Agilent G4477AA ChIP Analytics 1.3 software. The signal of a probe was converted into a "Me value", which represented the methylation level as a value from 0 (unmethylated) to 1 (methylated). Differentially methylated regions were detected by comparison between the Me values of two samples, and data were visualized in the UCSC Genome Browser (http://genome.ucsc.edu/) on NCBI36/hg18 assembly (National Center for Biotechnology Information, Bethesda, MD, USA).

Sodium bisulfite modification and quantitative methylation-specific polymerase chain reaction

Fully methylated DNA and fully unmethylated DNA were prepared by methylating genomic DNA with *SssI* methylase (New England Biolabs, Beverly, MA, USA) and by amplifying genomic DNA with the GenomiPhi amplification system (GE Healthcare, Buckinghamshire, UK), respectively. Bisulfite modification was performed using 1 μg of *Bam*HI-digested genomic DNA, and the modified

DNA was suspended in 40 μl of Tris–ethylenediamine tetraacetic acid (EDTA) buffer [16]. An aliquot of 2 μl of sodium bisulfite-treated DNA was used in one reaction of quantitative methylation-specific polymerase chain reaction (PCR; qMSP).

qMSP was performed using primer sets specific to methylated and unmethylated sequences (Supplementary Table 1), SYBR® Green I (BioWhittaker Molecular Applications, Rockland, ME, USA), and an iCycler Thermal Cycler (Bio-Rad Laboratories, Hercules, CA, USA). The number of molecules in a sample was determined by comparing its amplification with those of standard DNA that contained known numbers of molecules (10^1–10^9 molecules). Standard DNA was prepared by purifying the PCR products using the Wizard SV Gel and PCR Clean-Up System (Promega, Fitchburg, WI, USA). The methylation level was calculated as the fraction of methylated (M) molecules in the total number of DNA molecules (number of M molecules + number of unmethylated molecules). The percentage of methylated reference (PMR) was calculated as the fraction of the methylated reference {(number of M molecules in a sample)/(number of *Alu* repeat sequences in a sample)}/{(number of M molecules in *SssI*-treated DNA)/(number of *Alu* repeat sequences in *SssI*-treated DNA)} [17].

Statistical analysis

Differences in mean methylation levels or PMR were analyzed by the Student's *t*-test. The receiver-operating characteristic (ROC) curve was drawn, and the area under the curve (AUC) and OR were analyzed by binomial distribution and binomial logistic regression analysis, respectively. All the analysis was performed using PASW statistics (SPSS, Chicago, IL, USA), and the results were considered significant when *P* values of less than 0.05 were obtained by two-sided tests.

Results

Isolation of hypermethylated CGIs in GC-Pt compared with HV in individuals with past *H. pylori* infection

A pool of three samples from HV with past infection and another pool of three samples from GC-Pt with past infection were analyzed by MeDIP-CGI microarray analysis. CGIs that were hypermethylated in the latter group compared with the former group were selected as follows: (1) Me value in the latter pool was higher than that in the former pool by 0.2 or more, (2) Me value in the former pool was lower than 0.4, and (3) criteria (1) and (2) were satisfied in three consecutive probes. A total of 15 CGIs were isolated by these criteria (Table 1), and representative data around CGI #5 are shown in Fig. 1.

From the 15 CGIs, those differentially methylated in a screening set, which consisted of 10 HV with past infection and 10 GC-Pt with past infection, were searched for by evaluating PMRs by qMSP (Supplementary Table 2). Seven CGIs (#1 to #7; Table 1), distributed on various chromosomes, were methylated at significantly higher

Table 1 CGIs identified by MeDIP-CGI microarray

CGI no.	Gene symbol	Name	Chromosomal position	Location around a gene
#1	*EMX1*	Empty spiracles, homeobox 1	2p13.2	Intron 1
#2	*miR663*	MicroRNA 663	20p11.1	Overlap
#3	*NKX6-1*	NK6, homeobox 1	4q21.23	Intron 1
#4	*OTP*	Orthopedia homeobox	5q13.3	Downstream
#5	*OPLAH*	5-Oxoprolinase (ATP-hydrolysing)	8q24.3	Downstream
#6	*CYP1B1*	Cytochrome P450, family 1, subfamily B, polypeptide 1	2p22.2	Exon 1
#7	*NEFM*	Neurofilament, medium polypeptide	8p21	Exon 1
#8	*PMF1*	Polyamine-modulated factor 1	1q22	Intron 1
#9	*BDNF*	Brain-derived neurotrophic factor	11p14.1	Intron 1
#10	*SSTR5*	Somatostatin receptor 5	16p13.3	Promoter
#11	*MYO1D*	Myosin ID	17q11.2	Intron 1
#12	*CAMK2N2*	Calcium/calmodulin-dependent protein kinase II inhibitor 2	3q27.1	Promoter
#13	*GATA4*	GATA binding protein 4	8p23.1	Promoter
#14	*NFATC1*	Nuclear factor of activated T-cells, cytoplasmic, calcineurin-dependent 1	18q23	Promoter
#15	*ANKRD9*	Ankyrin repeat domain 9	14q32.31	Exon 1

CGI CpG island, *MeDIP* methylated DNA immunoprecipitation

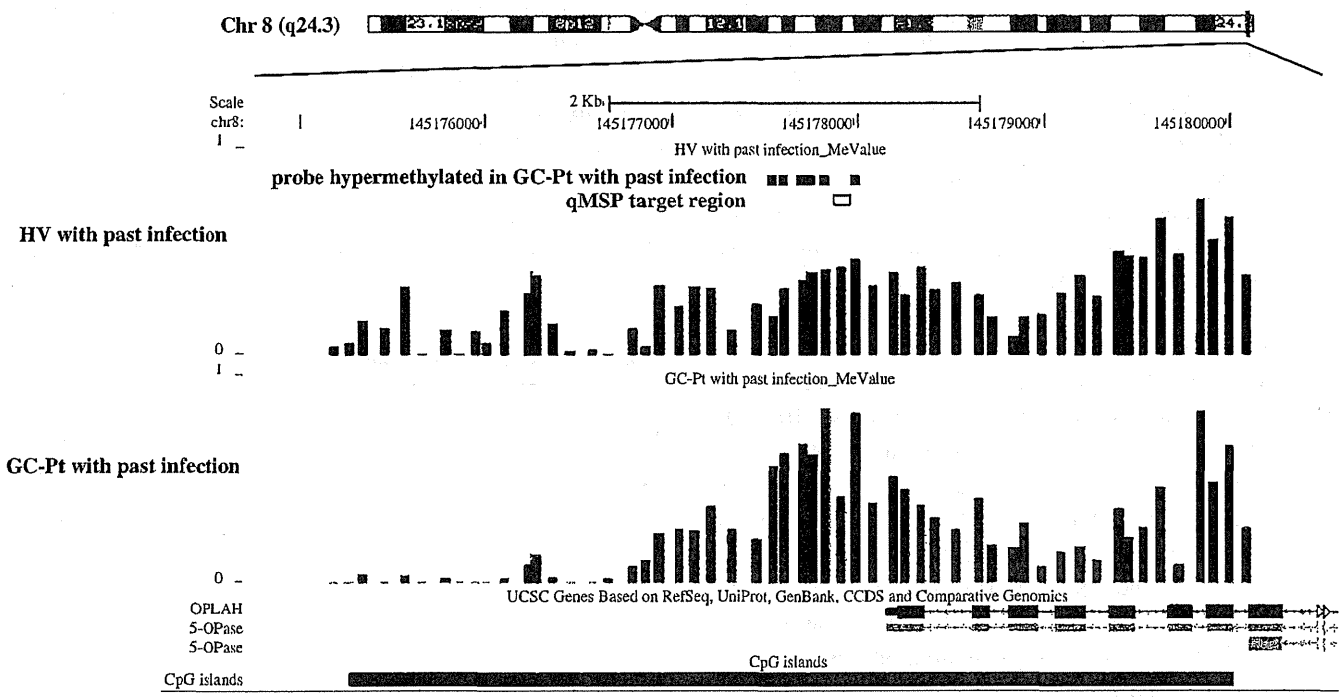

Fig. 1 Data of methylated DNA immunoprecipitation-CpG island (MeDIP-CGI) microarray analysis in the genomic region around CGI #5. Methylation levels were assessed by Me values, and the Me values of the two pools were visualized by the UCSC Genome Browser (http://genome.ucsc.edu/) for a genomic region (from nt. 145,174,733 to nt. 145,180,586 on chromosome 8 in NCBI36/hg18 assembly). *Vertical bars* show Me values of individual probes. *Closed boxes* above the Me values indicate the differentially methylated probes. Quantitative methylation-specific polymerase chain reaction (*qMSP*) primers were designed in the area shown by the *open box*. *HV* healthy volunteers, *GC-Pt* gastric cancer patients

levels in GC-Pt than in HV ($P < 0.05$). Relative positions against a gene also varied—two CGIs being located in exon 1, two in intron 1, two 300 bp downstream of the annotated end, and one overlapping with *pre-microRNA 663*.

Validation of the usefulness of the seven markers

The usefulness of the seven CGIs was validated by qMSP analysis of an independent set of samples (Fig. 2). The validation set consisted of seven never-infected HV (Group [G] 1), 21 HV with current infection (G2), 14 HV with past infection (G3), 21 GC-Pt with current infection (G4), and 21 GC-Pt with past infection (G5) (Supplementary Table 3). For comparison, two currently available markers (*FLNc* and *THBD*) were also analyzed. In the individuals with past infection (G3 and G5), the seven CGIs had levels that were 2.8-, 1.5-, 3.8-, 2.3-, 2.5-, 1.8-, and 3.8-fold, respectively, higher in G5 than in G3 ($P < 0.01$). *FLNc* tended to have a higher level in G5 than in G3 ($P = 0.087$), but *THBD* did not show any significant difference ($P = 0.341$). These data showed that the methylation levels of all the seven CGIs had the power of cancer risk estimation even in individuals with past infection.

In the HV, methylation levels in G2 were much higher than those in G1 ($P < 0.05$), but those in G3 were lower than those in G2. This observation supported the model that active infection by *H. pylori* induces methylation potently in non-stem cells, in addition to stem cells, and that methylation levels will eventually decrease after *H. pylori* infection has been eradicated. Also, methylation levels in G3 were significantly higher (four of the seven CGIs, $P < 0.05$) or tended to be higher than those in G1. This observation again supported the model that methylation induced in stem cells will remain even after *H. pylori* infection is eradicated.

Power of the seven CGIs as gastric cancer risk markers

AUCs to detect individuals in G5 were calculated using individuals in G3 and G5 (Table 2; Fig. 3). AUCs for the seven CGIs ranged between 0.78 and 0.84 and were significantly larger than 0.5 ($P < 0.01$). In contrast, the AUCs for the two currently available markers were 0.69 (95% CI 0.51–0.87) and 0.65 (95% CI 0.45–0.84), respectively, and were not significantly different from 0.5. Using optimal cut-off values obtained by the ROCs, ORs for the seven CGIs were calculated to be 12.7–36.0 (Table 2). ORs for

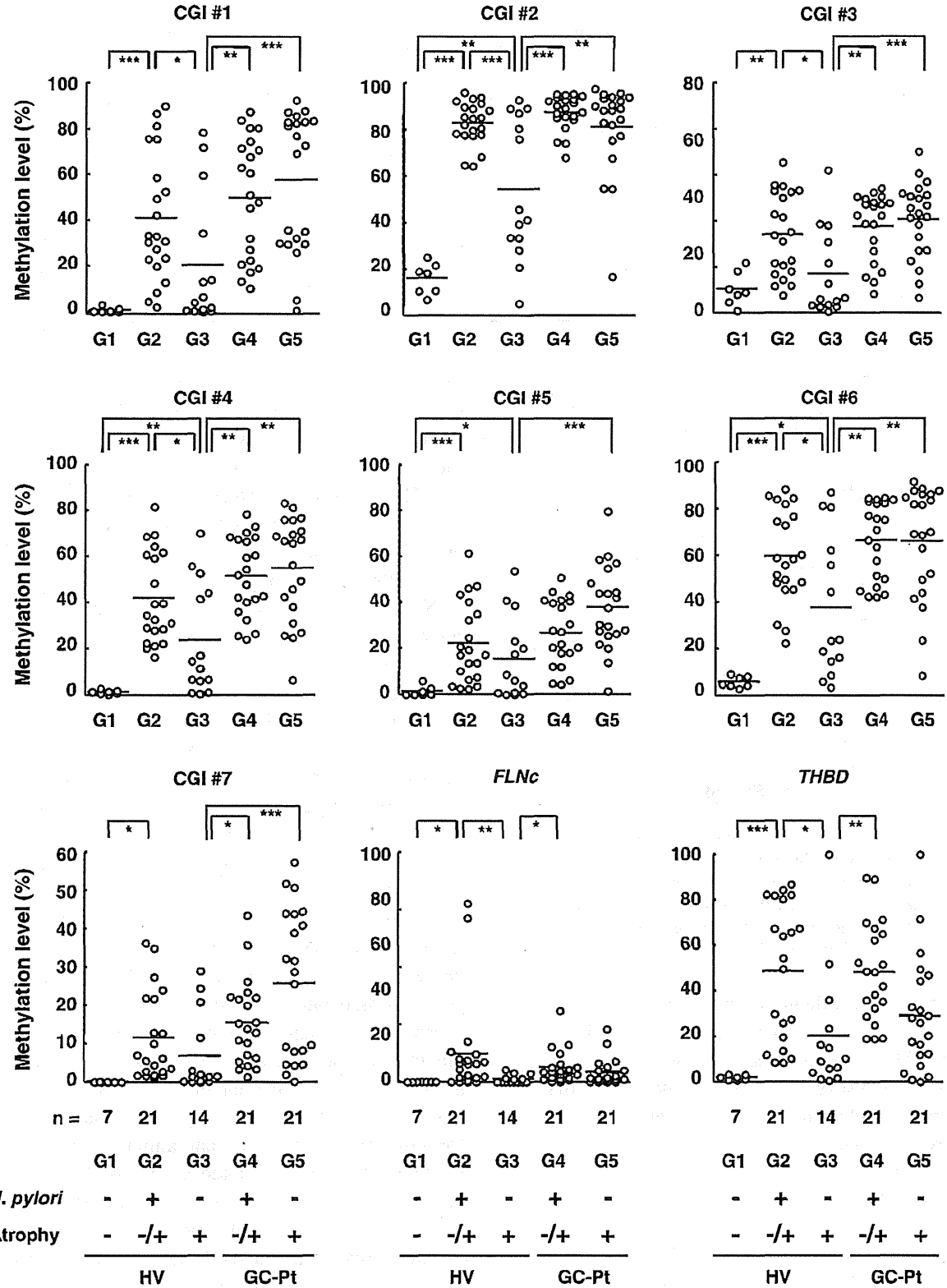

Fig. 2 Methylation levels of the seven CGIs and two currently available markers, *FLNc* and *THBD*, in the validation set. The *horizontal line* represents the mean methylation level in each group. Methylation levels of the seven CGIs in Group 5 (G5) were significantly higher than those in G3 ($P < 0.01$), but there were no significant differences for the two currently available markers. $^{*}P < 0.05$, $^{**}P < 0.01$, $^{***}P < 0.001$

Table 2 AUC and OR for new and currently available markers

CGI no.	Gene symbol	AUC	95% CI	*P* value	OR	95% CI	*P* value
#1	*EMX1*	0.84	0.70–0.97	<0.001	23.8	3.7–153	<0.001
#2	*miR663*	0.78	0.62–0.94	0.006	26.7	2.8–258	0.005
#3	*NKX6-1*	0.84	0.69–0.99	<0.001	15.0	2.8–80.1	0.002
#4	*OTP*	0.83	0.69–0.97	0.001	36.0	3.7–354	0.002
#5	*OPLAH*	0.83	0.69–0.98	0.001	15.6	2.9–83.5	0.001
#6	*CYP1B1*	0.78	0.62–0.94	0.006	12.7	2.1–76.7	0.006
#7	*NEFM*	0.84	0.71–0.98	<0.001	23.8	3.7–153	<0.001
–	*FLNc*	0.69	0.51–0.87	0.055	5.7	1.2–25.9	0.025
–	*THBD*	0.65	0.45–0.84	0.152	5.0	1.1–21.8	0.032

CGI CpG island, *AUC* area under the curve, *CI* confidence interval, *OR* odds ratio

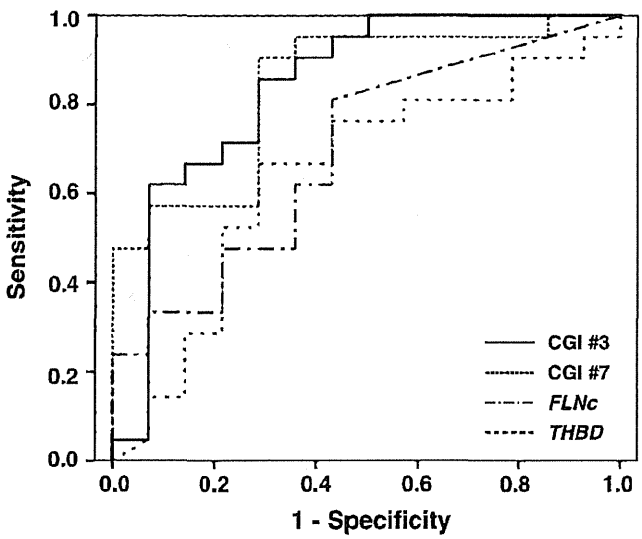

Fig. 3 Receiver-operating characteristic (ROC) curves of CGI #3 and #7, whose AUC values were the largest in the seven CGIs, are shown with those of two currently available markers, *FLNc* and *THBD*. *Black line*, *dotted line*, *dot-and-dash line*, and *dashed line* show ROC curves of CGI #3, #7, *FLNc*, and *THBD*, respectively. The AUC values of CGI #3 and #7 were larger than those of *FLNc* and *THBD*

the two currently available markers, *FLNc* and *THBD*, were 5.7 (95% CI 1.2–25.9) and 5.0 (95% CI 1.1–21.8), respectively. These results clearly showed that the methylation levels of the seven CGIs had greater power than the two currently available markers to estimate gastric cancer risk in individuals with past infection.

Discussion

In the present study, by carrying out genome-wide methylation analysis of gastric cancer patients (GC-Pt) and healthy volunteers (HV), both with past infection, we screened seven gastric cancer risk markers that are highly informative in individuals with past infection. Their usefulness was validated in 35 individuals (21 GC-Pt and 14 age-matched HV). To our knowledge, this is the first study that has evaluated epigenetic gastric cancer risk markers in individuals with past infection, and these markers are expected to be especially useful. This is because the number of individuals with past infection is increasing as more and more people receive *H. pylori* eradication therapy [18], but the usefulness of the current methods for gastric cancer risk estimation, i.e., a combination of the detection of *H. pylori* infection and the serum pepsinogen test, in this population has not been established [18–20].

None of the seven CGIs were located in promoter regions. We analyzed the association between the methylation levels of the seven CGIs and the expression levels of genes close to them, but no association was observed for any of the seven CGIs (data not shown). This was in line with the current knowledge that DNA methylation of only promoter CGIs consistently causes gene silencing, but that methylation of gene bodies may or may not be associated with increased expression [14, 21, 22]. The lack of association between methylation and gene expression supported the hypothesis that the methylation of these seven CGIs reflects the degree of overall epigenomic damage in gastric stem cells, and that the degree of epigenomic damage, and not the change of expression of individual genes, is associated with gastric cancer risk.

Epigenomic damage induced by *H. pylori* infection is one of the major causes of gastric cancer [23–26], but it is not known whether the epigenomic damage is independent of other risk factors. For example, salt intake is a risk factor for gastric cancer [27, 28], and although it does not induce methylation in gastric mucosae by itself in a Mongolian gerbil model [29, 30], it shows synergistic effects with *H. pylori* on cancer development [31]. It is not known yet whether epigenomic damage in the gastric mucosa provides independent information from past salt exposure or whether the exposure is already reflected in methylation levels. Multivariate analysis in a large cohort with a reliable record of history of salt intake will clarify this issue, and might provide a risk marker that complements the epigenetic gastric cancer risk markers.

In conclusion, we identified seven CGIs whose methylation levels are increased after *H. pylori* infection, and

are associated with gastric cancer risk even in individuals with past infection. These seven CGIs are promising candidate markers to estimate gastric cancer risk.

Acknowledgments This study was supported by Grants-in-Aid for Pioneering Basic Research and for the Third-term Comprehensive Cancer Control Strategy from the Ministry of Health, Labour and Welfare, Japan.

References

1. Uemura N, Okamoto S, Yamamoto S, Matsumura N, Yamaguchi S, Yamakido M, et al. *Helicobacter pylori* infection and the development of gastric cancer. N Engl J Med. 2001;345:784–9.
2. Forman D, Webb P, Parsonnet J. *H. pylori* and gastric cancer. Lancet. 1994;343:243–4.
3. Suzuki H, Iwasaki E, Hibi T. *Helicobacter pylori* and gastric cancer. Gastric Cancer. 2009;12:79–87.
4. Ekström AM, Held M, Hansson LE, Engstrand L, Nyrén O. *Helicobacter pylori* in gastric cancer established by CagA immunoblot as a marker of past infection. Gastroenterology. 2001;121:784–91.
5. El-Omar EM, Carrington M, Chow WH, McColl KE, Bream JH, Young HA, et al. Interleukin-1 polymorphisms associated with increased risk of gastric cancer. Nature. 2000;404:398–402.
6. Loh M, Koh KX, Yeo BH, Song CM, Chia KS, Zhu F, et al. Meta-analysis of genetic polymorphisms and gastric cancer risk: variability in associations according to race. Eur J Cancer. 2009;45:2562–8.
7. Maekita T, Nakazawa K, Mihara M, Nakajima T, Yanaoka K, Iguchi M, et al. High levels of aberrant DNA methylation in *Helicobacter pylori*-infected gastric mucosae and its possible association with gastric cancer risk. Clin Cancer Res. 2006;12:989–95.
8. Nakajima T, Enomoto S, Yamashita S, Ando T, Nakanishi Y, Nakazawa K, et al. Persistence of a component of DNA methylation in gastric mucosae after *Helicobacter pylori* eradication. J Gastroenterol. 2010;45:37–44.
9. Nakajima T, Maekita T, Oda I, Gotoda T, Yamamoto S, Umemura S, et al. Higher methylation levels in gastric mucosae significantly correlate with higher risk of gastric cancers. Cancer Epidemiol Biomarkers Prev. 2006;15:2317–21.
10. Ushijima T. Epigenetic field for cancerization. J Biochem Mol Biol. 2007;40:142–50.
11. Japanese Gastric Cancer Association. Japanese classification of gastric carcinoma—2nd English edition. Gastric Cancer. 1998;1:10–24.
12. Asaka M, Sugiyama T, Nobuta A, Kato M, Takeda H, Graham DY. Atrophic gastritis and intestinal metaplasia in Japan: results of a large multicenter study. Helicobacter. 2001;6:294–9.
13. Ohkusa T, Fujiki K, Takashimizu I, Kumagai J, Tanizawa T, Eishi Y, et al. Improvement in atrophic gastritis and intestinal metaplasia in patients in whom *Helicobacter pylori* was eradicated. Ann Intern Med. 2001;134:380–6.
14. Yamashita S, Hosoya K, Gyobu K, Takeshima H, Ushijima T. Development of a novel output value for quantitative assessment in methylated DNA immunoprecipitation-CpG island microarray analysis. DNA Res. 2009;16:275–86.
15. Takeshima H, Yamashita S, Shimazu T, Niwa T, Ushijima T. The presence of RNA polymerase II, active or stalled, predicts epigenetic fate of promoter CpG islands. Genome Res. 2009;16:275–86.
16. Kaneda A, Kaminishi M, Sugimura T, Ushijima T. Decreased expression of the seven ARP2/3 complex genes in human gastric cancers. Cancer Lett. 2004;212:203–10.
17. Weisenberger DJ, Campan M, Long TI, Kim MJ, Woods C, Fiala E, et al. Analysis of repetitive element DNA methylation by MethyLight. Nucleic Acids Res. 2005;33:6823–36.
18. Selgrad M, Bornschein J, Rokkas T, Malfertheiner P. Clinical aspects of gastric cancer and *Helicobacter pylori*—screening, prevention, and treatment. Helicobacter. 2010;15:40–5.
19. Kim N, Jung HC. The role of serum pepsinogen in the detection of gastric cancer. Gut Liver. 2010;4:307–19.
20. Mizuno S, Kobayashi M, Tomita S, Miki I, Masuda A, Onoyama M, et al. Validation of the pepsinogen test method for gastric cancer screening using a follow-up study. Gastric Cancer. 2009;12:158–63.
21. Hellman A, Chess A. Gene body-specific methylation on the active X chromosome. Science. 2007;315:1141–3.
22. Rauch TA, Wu X, Zhong X, Riggs AD, Pfeifer GP. A human B cell methylome at 100-base pair resolution. Proc Natl Acad Sci USA. 2009;106:671–8.
23. Rashid A, Issa JP. CpG island methylation in gastroenterologic neoplasia: a maturing field. Gastroenterology. 2004;127:1578–88.
24. Oue N, Motoshida J, Yokozaki H, Hayashi K, Tahara E, Taniyama K, et al. Distinct promoter hypermethylation of p16INK4a, CDH1, and RAR-beta in intestinal, diffuse-adherent, and diffuse-scattered type gastric carcinomas. J Pathol. 2002;198:55–9.
25. Shin CM, Kim N, Jung Y, Park JH, Kang GH, Kim JS, et al. Role of *Helicobacter pylori* infection in aberrant DNA methylation along multistep gastric carcinogenesis. Cancer Sci. 2011;101:1337–46.
26. Suzuki H, Tokino T, Shinomura Y, Imai K, Toyota M. DNA methylation and cancer pathways in gastrointestinal tumors. Pharmacogenomics. 2008;9:1917–28.
27. World Cancer Research Fund/American Institute for Cancer Research. Food, nutrition, physical activity, and the prevention of cancer: a global perspective. Washington, DC: AICR. 2007.
28. Nutrition and the prevention of chronic diseases. World Health Organ Tech Rep Ser. 2003;916:1–149.
29. Hur K, Niwa T, Toyoda T, Tsukamoto T, Tatematsu M, Yang HK, et al. Insufficient role of cell proliferation in aberrant DNA methylation induction and involvement of specific types of inflammation. Carcinogenesis. 2011;32:35–41.
30. Tatematsu M, Nozaki K, Tsukamoto T. *Helicobacter pylori* infection and gastric carcinogenesis in animal models. Gastric Cancer. 2003;6:1–7.
31. Nozaki K, Shimizu N, Inaba K, Tsukamoto T, Inoue M, Kumagai T, et al. Synergistic promoting effects of *Helicobacter pylori* infection and high-salt diet on gastric carcinogenesis in Mongolian gerbils. Jpn J Cancer Res. 2002;93:1083–9.

Cancer Letters 330 (2013) 33–40

Contents lists available at SciVerse ScienceDirect

Cancer Letters

journal homepage: www.elsevier.com/locate/canlet

Comprehensive DNA methylation and extensive mutation analyses reveal an association between the CpG island methylator phenotype and oncogenic mutations in gastric cancers

Jeong Goo Kim [a,b], Hideyuki Takeshima [a], Tohru Niwa [a], Emil Rehnberg [a], Yasuyuki Shigematsu [a], Yukie Yoda [a,c], Satoshi Yamashita [a], Ryoji Kushima [d], Takao Maekita [e], Masao Ichinose [e], Hitoshi Katai [c], Won Sang Park [f], Young Seon Hong [g], Cho Hyun Park [b,*], Toshikazu Ushijima [a,*]

[a] *Division of Epigenomics, National Cancer Center Research Institute, 5-1-1 Tsukiji, Chuo-ku, Tokyo 104-0045, Japan*
[b] *Department of Surgery, College of Medicine, The Catholic University of Korea, 222 Banpo-daero, Seocho-gu, Seoul 137-701, Republic of Korea*
[c] *Gastric Surgery Division, National Cancer Center Hospital, 5-1-1 Tsukiji, Chuo-ku, Tokyo 104-0045, Japan*
[d] *Pathology Division and Clinical Laboratory, National Cancer Center Hospital, 5-1-1 Tsukiji, Chuo-ku, Tokyo 104-0045, Japan*
[e] *Second Department of Internal Medicine, Wakayama Medical University, 811-1, Kimiidera, Wakayama 641-8509, Japan*
[f] *Department of Pathology, College of Medicine, The Catholic University of Korea, 222 Banpo-daero, Seocho-gu, Seoul 137-701, Republic of Korea*
[g] *Department of Internal Medicine, College of Medicine, The Catholic University of Korea, 222 Banpo-daero, Seocho-gu, Seoul 137-701, Republic of Korea*

ARTICLE INFO

Article history:
Received 10 October 2012
Received in revised form 12 November 2012
Accepted 12 November 2012

Keywords:
Epigenetics
Aberrant DNA methylation
CIMP
Mutation
Gastric cancer

ABSTRACT

Recent development of personal sequencers for extensive mutation analysis and bead array technology for comprehensive DNA methylation analysis have made it possible to obtain integrated pictures of genetic and epigenetic alterations on the same set of cancer samples. Here, we aimed to establish such pictures of gastric cancers (GCs). Comprehensive methylation analysis of 30 GCs revealed that the number of aberrantly methylated genes was highly variable among individual GCs. Extensive mutation analysis of 55 known cancer-related genes revealed that 19 of the 30 GCs had 24 somatic mutations of eight different genes (*CDH1*, *CTNNB1*, *ERBB2*, *KRAS*, *MLH1*, *PIK3CA*, *SMARCB1*, and *TP53*). Integration of information on the genetic and epigenetic alterations revealed that the GCs with the CpG island methylator phenotype (CIMP) tended to have mutations of oncogenes, *CTNNB1*, *ERBB2*, *KRAS*, and *PIK3CA*. This is one of the first studies in which both genetic and epigenetic alterations were extensively analyzed in the same set of samples. It was also demonstrated for the first time in GCs that the CIMP was associated with oncogene mutations.

© 2012 Elsevier Ireland Ltd. All rights reserved.

1. Introduction

Both genetic and epigenetic alterations are important for human carcinogenesis [1,2]. Genetic alterations are responsible for activation of oncogenes and inactivation of tumor-suppressor genes [2]. In human gastric cancers (GCs), oncogenes activated by mutations include *CTNNB1* (β-catenin), *ERBB2*, and *PIK3CA* [3–10], and tumor-suppressor genes inactivated by mutations include *CDH1* (E-cadherin), *CDKN2A* (*p16*), *TP53*, and *ARID1A* [11,12]. Even by whole exome sequencing of GCs, the vast majority of driver genes identified were known cancer-related genes, and novel genes identified, such as *ARID1A* and *FAT4*, had only low incidences of mutations [11,12]. This indicates that extensive mutation analysis of a large number of known cancer-related genes can provide an overall picture of a cancer sample, and this is now possible with high speed and low cost by using next-generation personal sequencers [13,14].

Epigenetic alterations, namely aberrant DNA methylation of promoter CpG islands (CGIs), are also responsible for inactivation of various tumor-suppressor genes [1]. DNA methylation statuses of the entire genome can be now comprehensively analyzed using microarray technologies, and bead array technology is especially useful for its quantitative measurement [15]. In GCs, tumor-suppressor genes inactivated by promoter methylation include *CDH1*, *CDKN2A*, *FHL1*, *LOX*, *MLH1*, and *SFRP* family genes (*SFRP1*, *SFRP2*, and *SFRP5*) [16–21]. These tumor-suppressor genes are more frequently inactivated by aberrant methylation than by genetic alterations in GCs [22]. In addition, aberrant methylation is induced in gastric mucosae by *Helicobacter pylori* (*H. pylori*)

Abbreviations: GC, gastric cancer; CGI, CpG island; *H. pylori*, *Helicobacter pylori*; CIMP, CpG island methylator phenotype; EB virus, Epstein–Barr virus; TSS, transcription start site; COSMIC, Catalogue Of Somatic Mutations In Cancer.

* Corresponding authors. Fax: +81 3 5565 1753.
E-mail address: tushijim@ncc.go.jp (T. Ushijima).

0304-3835/$ - see front matter © 2012 Elsevier Ireland Ltd. All rights reserved.
http://dx.doi.org/10.1016/j.canlet.2012.11.022

infection [23,24], a well-established major inducer of human GCs [25]. The frequent inactivation of tumor-suppressor genes by aberrant methylation and the deep involvement of *H. pylori* infection in its induction indicate the importance of epigenetic alterations in GCs.

Not only in GCs but also in other types of cancers, a subgroup of cancers is known to have frequent aberrant DNA methylation of CGIs, referred to as the CpG island methylator phenotype (CIMP). The CIMP was first described in colorectal cancers [26], and is associated with unique clinicopathological features. For example, the CIMP is associated with poor prognosis in colorectal cancers, lung cancers, and neuroblastomas [27–29]. In contrast, depending on the number and set of genes used for the determination of the CIMP status, the CIMP can be associated with either poor or good prognosis in GCs [30–33]. The CIMP in specific cancers is associated with genetic alterations, such as mutations of *BRAF*, *KRAS*, and *PIK3CA* in colorectal cancers [34–37], and amplification of *ERBB2* in breast cancers [38]. In contrast, little is known on a specific association between the CIMP and genetic alterations in GCs.

In this study, we aimed to establish integrated pictures of genetic and epigenetic alterations of GCs. To this end, we conducted comprehensive analysis of DNA methylation statuses using bead array technology, and extensive analysis of mutations of 55 known cancer-related genes using a next-generation personal sequencer.

2. Materials and methods

2.1. Samples

Thirty GC samples were obtained from patients who underwent gastrectomy with informed consents. Three normal gastric mucosae samples were obtained endoscopically from healthy volunteers without *H. pylori* infection with informed consents. The study was approved by the Institutional Review Boards. The samples were stored in RNAlater (Life Technologies, Carlsbad, CA) at −80 °C until the extraction of genomic DNA (GC samples and normal gastric mucosae samples) and RNA (normal gastric mucosae samples). Clinical information of the 30 GCs is shown in Supplementary Table 1. The status of Epstein–Barr (EB) virus infection was evaluated by PCR using primers specific to genomic DNA of EB virus (forward, CGGTATTATGTTTTTGGTATGTGTA; reverse, ATAACAACAACGTCATAAAAACCAC), and no infection was present in the 30 GCs.

Genomic DNA was extracted from GC and normal gastric mucosae samples by the phenol/chloroform method, and was quantified by using a Quant-iT PicoGreen dsDNA Assay Kit (Life Technologies). Total RNA was isolated using ISOGEN (Nippon Gene, Tokyo, Japan).

2.2. Analysis of DNA methylation

Analysis of DNA methylation was performed using an Infinium HumanMethylation450 BeadChip array, which covered 482,421 CpG sites (Illumina, San Diego, CA) as described previously [39]. CpG sites with low signals (signal <500, 0.19–2.19% of total CpG sites) were excluded from further analyses. The methylation level of each CpG site was represented by β values which ranged from 0 (unmethylated) to 1 (fully methylated).

A total of 193,531 genomic "segments" were defined by their location against a transcription start site (TSS) [TSS1500 (regions between 200 bp upstream and 1500 bp upstream from TSS), TSS200 (200 bp upstream region from TSS), 5′-UTR, 1st exon, gene body, 3′-UTR, and intergenic regions] and their relative location against a CGI (N Shelf, N Shore, CGI, S Shore, S Shelf, and non-CGI). A genomic segment >500 bp was further divided into genomic "blocks". A genomic block was defined as a 500-bp region from an initial CpG site (probe), and the next genomic block started from the next CpG site (Supplementary Fig. 1). A genomic segment ⩽500 bp was counted as one genomic block. A total of 282,805 genomic blocks were produced, and 276,456 genomic blocks on autosomes were analyzed to enable comparison between males and females. A DNA methylation level of a genomic block was evaluated using the average of β value of the CpG sites within the block. A genomic block was considered as methylated when its β value was 0.4 or more, and as unmethylated when its β value was 0.2 or less.

2.3. Analysis of sequence variations

A library DNA containing 226 amplicons of 55 cancer-related genes was prepared from a sample by multiplex PCR using 50 ng of genomic DNA and an Ion *AmpliSeq* Cancer Panel Kit (Life Technologies) with 36 customized primers (Supplementary Table 2). The 226 amplicons covered the vast majority of samples with mutations reported (91.9% or more) for 15 oncogenes and the *TP53* tumor-suppressor gene (83.1%), and variable fractions of samples with mutations reported (3.3–88.5%) for 39 genes (Supplementary Table 3). Then, the entire library DNA was uniquely barcoded by using an Ion Xpress Barcode Adaptors 1-16 Kit (Life Technologies). The barcoded libraries from five to six samples were pooled, and mixed with Ion Spheres for emulsion PCR using the Ion OneTouch System (Life Technologies) with an Ion OneTouch Template Kit (Life Technologies). From the product of emulsion PCR, the complexes of Ion Spheres with amplified DNA were enriched by using Ion OneTouch ES (Life Technologies) and were loaded onto an Ion 316 chip (Life Technologies). Sequencing was performed by using Ion PGM Sequencer (Life Technologies) with an Ion Sequencing Kit (Life Technologies). Obtained sequences were mapped onto the human reference genome hg19, and sequence variations with frequencies of 10% or more were identified by using CLC Genomics Workbench 5.1 (CLC bio, Aarhus, Denmark). Common SNPs were excluded from further analysis. Reading depths of individual regions analyzed are shown in Supplementary Table 4.

2.4. Dideoxy sequencing

A region containing a sequence variation identified was amplified using 20 ng of genomic DNA with primers listed in Supplementary Table 5. The PCR product was purified by a DNA Clean and Concentrator-5 Kit (Zymo Research, Irvine, CA), and directly cycle-sequenced by using a DYEnamic ET Terminator Cycle Sequencing kit (GE Healthcare, Buckinghamshire, UK) and an ABI PRISM 310 automated DNA sequencer (PE Biosystems).

2.5. Analysis of gene expression by GeneChip oligonucleotide microarray

Gene expression levels in normal gastric mucosae were analyzed by using the GeneChip Human Genome U133 Plus 2.0 microarray (Affymetrix, Santa Clara, CA) as described [40]. Genes with signal intensities of 250 or more were defined as expressed genes.

2.6. Cluster analysis

Unsupervised hierarchical clustering analysis was performed by using R 2.15 [R Core Team (2012) R: A language and environment for statistical computing. R Foundation for Statistical Computing, Vienna, Austria. ISBN 3-900051-07-0, URL http://www.R-project.org/] with the Heatplus package [Alexander Ploner (2011) Heatplus: Heatmaps with row and/or column covariates and colored clusters, R package version 2.2.0.] from Bioconductor [41]. The Euclidean distance was used as distance function both for samples and genes. Due to the limitation in the calculation algorithm for the hierarchical clustering, 25,000 elements or less were analyzed.

2.7. Survival curve

Survival curves were analyzed using the Kaplan-Meier method, and the Kaplan-Meier curve was drawn by using SPSS 13.0J (SPSS, Chicago, IL, USA).

2.8. Statistical analysis

The association between the CIMP and oncogene mutations, and that between genes aberrantly methylated in GCs and target genes of polycomb repressive complex (PRC) 2 in human embryonic stem (ES) cells were tested by the chi-square test. The differences in the survival rates among groups were evaluated using the Mantel-Cox test.

3. Results

3.1. Comprehensive analysis of DNA methylation profiles

DNA methylation levels were compared between GCs and normal gastric mucosae. First, using all the 276,456 genomic blocks, some GCs, such as S24TP, S33TP, and S37TP, had a larger fraction of aberrantly methylated blocks than other GCs, such as S2TP, S4TP, and S15TP (Fig. 1 and Supplementary Fig. 2). Second, the analysis was conducted using 6877 TSS200 CGIs unmethylated in normal gastric mucosae (genes unmethylated in normal gastric mucosae) because a TSS200 CGI is known to play a critical role in methylation-silencing [42]. The number of aberrantly methylated genes ranged from three to 1211. Third, we focused on TSS200 CGIs of genes with positive expression in normal cells but aberrantly methylated in cancer cells because this group of genes is known to frequently contain driver genes in carcinogenesis [43]. Using 263 TSS200 CGIs whose downstream genes were expressed in

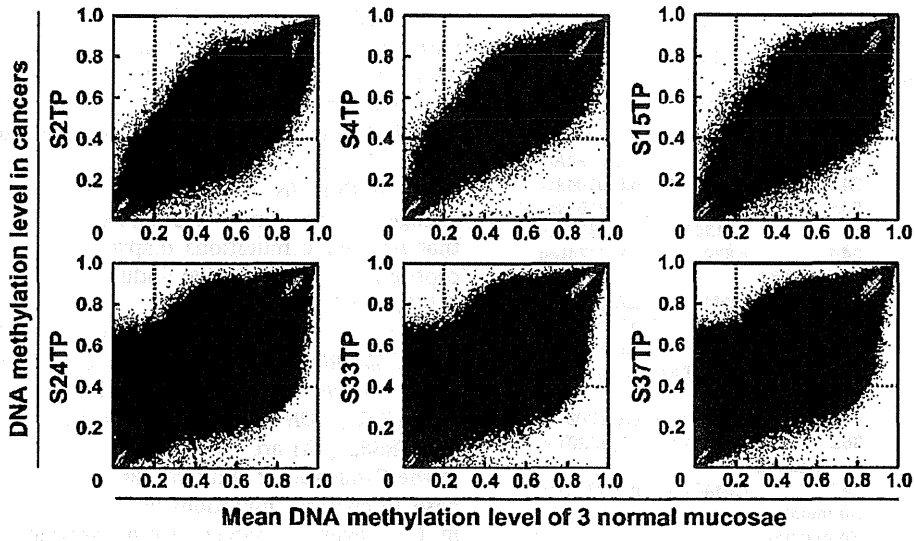

Fig. 1. Comprehensive analysis of DNA methylation profiles in GCs. DNA methylation levels were compared between GCs and normal gastric mucosae for the 276,456 genomic blocks. S24TP, S33TP, and S37TP (lower three panels) had a larger fraction of aberrantly methylated genes (yellow-colored areas) than S2TP, S4TP, and S15TP (upper three panels). The vertical and horizontal axes indicate the methylation levels in GCs and the mean methylation levels of three normal mucosae, respectively.

normal gastric mucosae and aberrantly methylated in one or more GCs (methylation-silenced genes), the number ranged from 0 to 166. These results showed that the number of aberrantly methylated genes was highly variable among individual GCs.

3.2. Extensive mutation analysis of the 55 cancer-related genes

Mutations were analyzed for the 55 cancer-related genes. Among the 30 GCs, 22 GCs had 30 sequence variations of at least one gene (Table 1 and Supplementary Table 6), and all the 30 sequence variations were confirmed by dideoxy sequencing (Supplementary Fig. 3). The confirmed sequence variations were analyzed whether or not they were somatic mutations using corresponding non-cancerous tissues. The 24 of the 30 sequence variations were shown to be somatic mutations (Fig. 2 and Table 1), and were present in 19 GCs. Among the 24 mutations, 22 were missense mutations, and two were nonsense mutations. Three GCs (S5TP, S13TP, and S33TP) had two or more mutations of different genes. Four oncogenes, *CTNNB1*, *ERBB2*, *KRAS*, and *PIK3CA*, and four tumor-suppressor genes, *CDH1*, *MLH1*, *SMARCB1*, and *TP53*, were mutated. *TP53* was most frequently mutated (43%, 13 of the 30 GCs), and *CTNNB1*, *ERBB2*, *KRAS*, and *PIK3CA* were mutated in two GCs. These results showed that 63% of GCs (19 out of the 30 GCs) had at least one somatic mutation of known cancer-related genes.

3.3. The association between the CIMP and mutations of oncogenes

Unsupervised hierarchical clustering analysis was conducted first using DNA methylation profiles of 25,000 genomic blocks randomly selected from all the 276,456 genomic blocks. However, the numbers of aberrantly methylated genes in GCs of different clusters did not appear to be different (Supplementary Fig. 4). Then, we again conducted unsupervised hierarchical clustering using DNA methylation profiles of CGIs, namely 25,000 genomic blocks randomly selected from 59,992 blocks with CGIs (Fig. 3A). This time, clusters I ($n = 3$) and IIb ($n = 13$) contained GCs with a larger number of aberrantly methylated genes than GCs in cluster IIa ($n = 14$). Among the 16 GCs in clusters I and IIb, seven GCs were shown to have mutations of oncogenes, *CTNNB1*, *ERBB2*, *KRAS*, and *PIK3CA*.

Thirdly, using DNA methylation profiles of 6877 genes unmethylated in normal gastric mucosae, two major clusters were observed (Fig. 3B). Cluster III ($n = 11$) contained GCs with a relatively large number of aberrantly methylated genes, and seven of the 11 GCs of this cluster were shown to have mutations of oncogenes, *CTNNB1*, *ERBB2*, *KRAS*, and *PIK3CA*. In contrast, cluster IV ($n = 19$) contained GCs with a relatively small number of aberrantly methylated genes, and none of the 19 GCs in this cluster had mutations of oncogenes. The difference was markedly statistically significant ($P = 7.15 \times 10^{-5}$), and GCs in cluster III and IV were considered to be the CIMP-positive [CIMP(+)] and the CIMP-negative [CIMP(−)], respectively.

Fourth, using DNA methylation profiles of the 263 methylation-silenced genes, three major clusters were produced (Fig. 3C). Cluster V ($n = 3$) contained GCs with the largest number of aberrantly methylated genes, and two of the three GCs were shown to have mutations of *PIK3CA*. Cluster VIa ($n = 8$) contained GCs with a relatively larger number of aberrantly methylated genes than GCs in cluster VIb ($n = 19$). Five of the eight GCs in this cluster were shown to have mutations of oncogenes, *CTNNB1*, *ERBB2*, *KRAS*. Clusters VIb contained the same sets of GCs as cluster IV, the previous clustering, except for one. These results showed that the CIMP(+) GCs were associated with mutations of oncogenes, such as *CTNNB1*, *ERBB2*, *KRAS* and *PIK3CA*, in GCs.

3.4. Possible association between the CIMP and good prognosis

To analyze an association between the CIMP status and prognosis of patients, Kaplan-Meier curves were drawn using overall survival (OS). Using the CIMP status based on the DNA methylation of the 6877 genes unmethylated in normal gastric mucosae, it was revealed that the prognosis of the CIMP(+) patients (Cluster III in Fig. 3B) tended to be better than that of the CIMP(−) patients (Cluster IV in Fig. 3B) ($P = 0.285$; Fig. 4). Also, using the CIMP status based on the methylation of the 263 methylation-silenced genes, the prognosis of the CIMP(+) patients (Cluster V and VIa in Fig. 3C) tended to be better than that of the CIMP(−) patients (Cluster VIb in Fig. 3C) ($P = 0.285$; Supplementary Fig. 5). These results suggested that the CIMP(+) status is possibly associated with good prognosis in GCs.

Table 1
List of somatic mutations identified in the 30 GCs.

Sample #	Sample name	Gene	Coverage	Variant frequencies	Nucleotide change	Amino acid change
1	S1TP	*CDH1*	339	10.3	c.1198G > A	p.Asp400Asn
2	S2TP	*TP53*	496	34.1	c.581T > G	p.Leu194Arg
3	S4TP	*TP53*	438	74.2	c.581T > G	p.Leu194Arg
4	S5TP	*KRAS*	1626	54.4	c.38G > A	p.Gly13Asp
		SMARCB1	50	56	c.1130G > A	p.Arg377His
5	S6TP	*TP53*	2077	24.7	c.820G > C	p.Val274Leu
6	S9TP			No mutation		
7	S11TP	*TP53*	10,211	53.4	c.844C > T	p.Arg282Trp
8	S12TP	*ERBB2*	24,516	63.8	c.2264T > C	p.Leu755Ser
9	S13TP	*TP53*	70	15.7	c.478A > G	p.Met160Val
		ERBB2	482	23.9	c.2264T > C	p.Leu755Ser
10	S14TP			No mutation		
11	S15TP	*TP53*	534	40.3	c.743G > A	p.Arg248Gln
12	S16TP	*TP53*	453	36.2	c.660T > G	p.Tyr220Ter
13	S17TP			No mutation		
14	S18TP	*TP53*	1946	26.5	c.844C > T	p.Arg282Trp
15	S19TP			No mutation		
16	S20TP			No mutation		
17	S22TP			No mutation		
18	S23TP	*TP53*	565	67.8	c.537T > A	p.His179Gln
19	S24TP			No mutation		
20	S32TP			No mutation		
21	S33TP	*MLH1*	4092	45.4	c.1744C > G	p.Leu582Val
		CTNNB1	11,994	20.5	c.101G > A	p.Gly34Glu
		PIK3CA	276	49.3	c.1633G > A	p.Glu545Lys
		TP53	1142	34.9	c.524G > A	p.Arg175His
22	S34TP	*TP53*	551	28.3	c.641A > G	p.His214Arg
23	S35TP	*KRAS*	770	41.3	c.35G > T	p.Gly12Val
24	S36TP	*TP53*	1142	34.9	c.524G > A	p.Arg175His
25	S37TP	*PIK3CA*	59	15.3	c.1624G > A	p.Glu542Lys
26	S40TP			No mutation		
27	S42TP			No mutation		
28	S43TP	*TP53*	239	74.9	c.1024C > T	p.Arg342Ter
29	S45TP			No mutation		
30	S47TP	*CTNNB1*	4591	33.7	c.121A > G	p.Thr41Ala

3.5. Association between the genes aberrantly methylated in GCs and genes targeted by PRC2 in ES cells

The fraction of genes targeted by PRC2 in ES cells was analyzed in the genes aberrantly methylated in GCs and those unmethylated in GCs because genes methylated in GCs were reported to be associated with PRC2 target genes [33]. Using the information on the PRC2 target genes in human ES cells [44,45], it was shown that the genes aberrantly methylated in GCs consisted of a larger fraction of PRC2 target genes than those unmethylated in GCs ($P = 6.64 \times 10^{-79}$) (Supplementary Fig. 6). These results confirmed that genes aberrantly methylated in GCs were associated with genes targeted by PRC2 in ES cells.

4. Discussion

In this study, we conducted comprehensive DNA methylation analysis and extensive mutation analysis of 30 GCs, and showed (1) that the number of aberrantly methylated genes was highly variable among the 30 GCs, (2) that 19 of the 30 GCs had 24 somatic mutations of 8 different genes (*CDH1*, *CTNNB1*, *ERBB2*, *KRAS*, *MLH1*, *PIK3CA*, *SMARCB1*, and *TP53*), and (3) that the CIMP was associated with mutations of oncogenes, including *ERBB2*, *CTNNB1*, *KRAS*, and *PIK3CA*, in GCs. This is one of the first studies in which both genetic and epigenetic alterations were extensively analyzed in the same set of samples, and the association between the CIMP and mutations of oncogenes in GCs was revealed here for the first time.

A similar association has been known also in colorectal cancers, but the mechanisms for this association are still unclear. As a possible mechanism, it has been proposed (1) that cancers with the CIMP can escape senescence caused by *BRAF* mutation owing to silencing of regulators of senescence by *BRAF* mutation, such as *IGFBP7* [46,47], and (2) that overexpression of the *BRAF* mutant can induce aberrant methylation at various genes, such as *MLH1* [48]. Similar possibilities can be hypothesized in GCs. As a mechanism for methylation induction by oncogenic mutation, if this applies to GCs, there is a possibility that oncogenic mutations displace factors involved in the susceptibility to methylation induction, such as RNA polymerase II [40,49–53].

Somatic mutations of four tumor-suppressor genes, *CDH1*, *MLH1*, *SMARCB1*, and *TP53*, and four oncogenes, *CTNNB1*, *ERBB2*, *KRAS*, and *PIK3CA*, were identified. Among these mutated genes, *TP53* (32%), *CDH1* (20%), *PIK3CA* (10%), *CTNNB1* (9%), *KRAS* (7%), and *ERBB2* (2%) are listed in the top 15 mutated genes in GCs in the Catalogue Of Somatic Mutations In Cancer (COSMIC) database. In contrast, mutations of *SMARCB1* have not been identified in GCs, even by whole exome sequencing [11,12], but were identified for the first time in this study, showing the usefulness of extensive mutation analysis of known cancer-related genes. *SMARCB1* encodes a component of chromatin remodeling complex, SWI/SNF, and is mutated in malignant rhabdoid tumors [54]. In GCs, the defects of components of SWI/SNF, such as mutation of *ARID1A* [11,12] and loss of BRM expression, are known [55]. Therefore, it is considered that the dysfunction of chromatin remodeling activity plays an important role in gastric carcinogenesis.

The selection of genomic blocks heavily influenced the results of unsupervised hierarchical clustering analysis. The association between the CIMP and mutations of oncogenes was clearly observed using DNA methylation profiles of the selected 6877 and 263 blocks, and some association was observed using the methylation profiles of the 25,000 blocks with CGIs. In contrast, no association was observed using the 25,000 blocks randomly selected from all the blocks. Therefore, it is considered that the selection of biologically important probes (or genes) is required to extract meaningful information from the huge amount of data obtained by comprehensive DNA methylation analysis.

We previously found that the CIMP statuses in GCs were not associated with DNA methylation statuses in background non-cancerous mucosae, contrary to expectations [30]. The presence of the CIMP(+) GCs suggested that CGIs methylated in GCs are composed of those methylated as a result of the CIMP and those methylated in background non-cancerous mucosae.

The genes aberrantly methylated in GCs here were associated with genes targeted by PRC2 in ES cells, confirming previous reports. It has been known that genes methylated in other types of cancers are associated with genes targeted by PRC2 in ES cells [49,50,53] or normal cells [40,50–52]. A recent comprehensive analysis in GCs also revealed that genes methylated in GCs were associated with genes targeted by PRC2 in ES cells [33]. EZH2, a component of PRC2, and CBX7, a component of PRC1, are known to interact with DNA methyltransferases [56,57], and these interactions seem to be a possible mechanism of the high frequency of DNA methylation of the genes targeted by PRC2.

The prognosis of the CIMP(+) patients tended to be better than that of the CIMP(−) patients. The association between the CIMP and prognosis is highly dependent upon cancer types. For example, the CIMP is associated with poor prognosis in colorectal cancers [28], lung cancers [29], and neuroblastoma [27]. In GCs, some studies showed association with good prognosis [30,31], and others showed that with poor prognosis [32,33]. The reason why the CIMP in GCs was associated with good prognosis in some studies is unknown, but it might be possible that genes involved